FAST-IOTA ROOKIE BOOK

By Darren J. Crawford

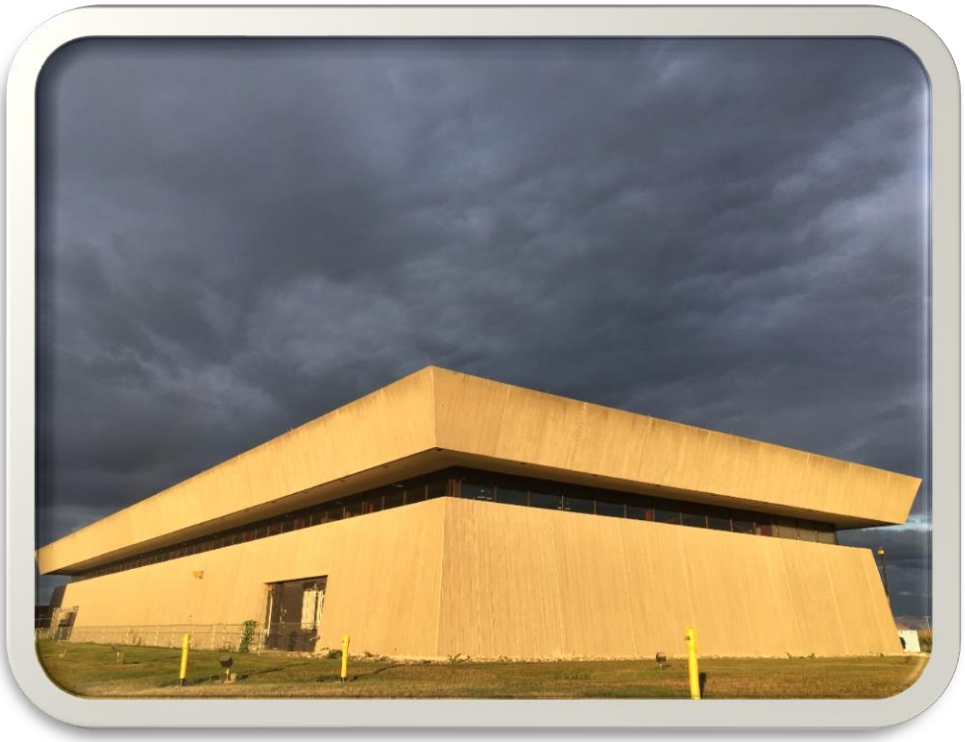

Fermilab Accelerator Science & Technology Facility

Introduction

NML is the home of the Fermilab Accelerator Science and Technology (FAST) facility and the Integrable Optics Test Accelerator (IOTA) which is a part of the Accelerator Science and Technology (AST) sector. The FAST Facility Department is located at NML, see front cover. FAST began as a superconducting RF cryomodule test facility utilizing International Linear Collider (ILC) funds. The facility has cryogenics, LCW, ICW, and vacuum systems. The Cave enclosure, Figure i, houses the electron source, which utilizes a laser liberating electrons from the surface of a Cesium Telluride (Cs_2Te) coated Molybdenum plug via the photo-electric effect. An RF gun accelerates the photo-electrons to Capture Cavity 1 and 2 (aka CC1 and CC2). These two cavities accelerate the electron beam up to 55 MeV. The Low Energy Beamline following the capture cavities is used for determining the emittance and position of the beam as well as compressing and transforming the shape. The beam energy can be measured when it is directed through a spectrometer magnet at the low energy absorber (LEA). The High Energy Beamline begins at a quadrupole triplet immediately upstream of Cryomodule 2 (CM2). CM2 consists of eight 9-cell superconducting niobium cavities and provides a net energy gain of 250 MeV. All cavities operate at 1.3 GHz. The exiting beam is transported through the High Energy Beamline. There is a beam dump at the end of the beamline, which utilizes a graphite absorber bathed in helium, encased in aluminum, and water cooled via a dedicated skid.

The Integrable Optics Test Accelerator (IOTA) is a storage ring for advanced beam physics research and is located at the downstream end of the High Energy Beamline. It will operate with protons and electrons using injectors with momenta of 70 and 150 MeV/c, respectively. The research program includes the study of nonlinear focusing integrable optical beam lattices based on special magnets and electron lenses, beam dynamics of space-charge effects and their compensation, optical stochastic cooling, and several other experiments.

Thanks to Chip Edstrom, Kermit Carlson, Jamie Santucci, Yurick Czajkowski, Mark Obrycki, and Sasha Valishev for their help, in various ways, with this rookie book.

Figure i. Inside NML, over the south end of the Cave, looking northward (downstream).

SECTION 1

DESIGN AND LAYOUT OF THE ELECTRON LINAC

The FAST electron linac comprises a number of components, including a UV Drive Laser, 5 MeV RF Gun, a set of capture cavities, a 25 meter long low energy (≤55 MeV) beamline, a cryomodule, and a ~100 meter long high energy (≤300 MeV) beamline.

1.1 UV Drive Laser

The FAST laser system is housed in a dedicated, temperature and humidity controlled 8.7 m x 6.5 m room on the FAST hall floor adjacent to the beamline enclosure, commonly called the laser room. There are 3 optical tables inside the laser room – one table dedicated to the photocathode laser, one table intended for a high bandwidth Ti:Sa laser, and one table intended for future laser R&D. The UV laser light is transported into the tunnel enclosure via an evacuated pipe with 2 mirror boxes.

Construction of the laser room at the FAST facility in NML was completed near the beginning of the August 2012. UV laser pulses were produced by the end of 2012. The FAST laser system interface is a synoptic display, which is a client-server system for graphical data representation through the Fermilab accelerator control system, ACNET. As such, it is similar to other GUI packages such as ACNET Lex SA, EPICS EDM, and DESY JDDD. In addition to ease of development, and a modern look and feel, live synoptic pages can be viewed as SVG, PNG, or other web-friendly formats through most common web browsers with relatively low use of bandwidth. More details about the laser control interface can be found in (Dean R. Edstrom Jr et. al., "GUI Development for the Drive Laser at Fermilab's FAST Facility", IPAC'14, Dresden, Germany, June 2014).

The laser system for the RF Gun photocathode has three stages. The first stage is an infrared (IR) laser (λ=1054 nm) generated from a fiber-based seed laser. The IR laser goes through a chain of amplifications and is then frequency doubled into a green laser (stage 2). The third and final stage is to frequency double the green laser from 527 nm to 263.5 nm, which is in the UV portion of the electro-magnetic spectrum. The Class 4, 25 μJ/pulse laser is directed into an evacuated pipe and reflected to the Cathode Optics Box (COB) on the Diagnostic table immediately downstream of the RF Gun. Figure 1-1 below is the designed flow chart of the entire photocathode laser system and

shows the progression of the laser from the IR seed laser in the top left box through the chain of solid-state amplifiers and frequency multiplication to UV in the bottom right box. Expected power levels are given at each stage.

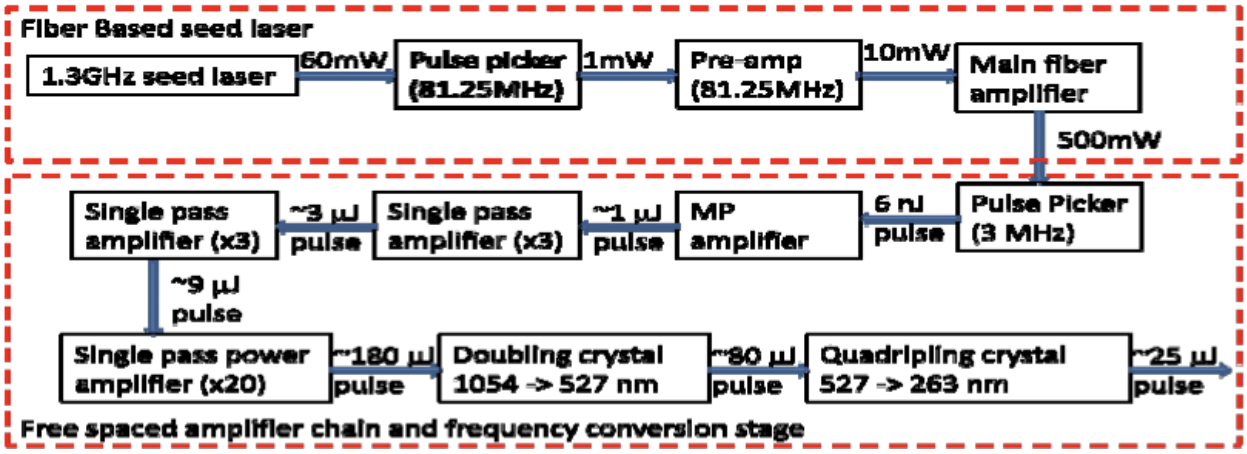

Figure 1-1. UV Drive Laser system flow chart.

1.1.1 System design

The FAST laser system is based on the design used for many years at the A0 photoinjector, with some notable improvements. One of the disadvantages of the A0 laser system design was the low efficiency of the gain medium, Nd:Glass, used in the amplifying structure. Coupled with the fact that the flash lamp used to pump the gain medium is relatively unstable, it is difficult to realize long pulse train operation as required in FAST with such a system. In order to address this issue FAST is using Neodymium-doped yttrium–lithium fluoride (Nd:YLF) as the gain medium to replace the Nd:glass used in previous A0 laser amplifier chain. Nd:YLF is a very efficient material that can be pumped by either flash lamp or diode laser. In addition, the induced emission cross section is large enough to produce a single pass amplification up to a factor of 10. At the same time the flash lamp pump was changed to a fiber coupled laser diode pump to get better stability and higher reliability. Using optical fiber to deliver the pump to the end-pumped active medium has several practical advantages:

- The pump beam at the end of the fiber has a high quality, central symmetrical profile.
- The radial size of the beam can be easily scaled up or scaled down with high quality optics.
- A fiber connection provides a simple and virtually lossless interface between the pump source and the active medium.
- Both the pump source and active medium can be changed simply by reconnecting the fiber between them.

In addition to changing the amplifying chain we also replaced the solid state seed laser used at A0 with a fiber laser based seed system. The solid-state seed laser is kept as a backup.

1.1.2 Fiber-Based Seed Laser

This system was designed and built at Calmar Laser Inc. Figure 1-2 is a photo of the entire system. The seed laser is an active mode locked Yb-fiber laser system centered at 1054 nm. The laser cavity consists of yttrbium doped fiber amplifier (YDFA), output coupler, electro-optics modulator, tunable filter and fibers that connect these devices together. A piezo stage is used to adjust the cavity length to achieve stable mode-locking. The pulse width is 3.2 ps RMS as measured with an auto-correlator, and the laser is phase-locked to a 1.3 GHz signal from the low level RF master oscillator. The modulator bias voltage needs to be adjusted to a proper DC value to ensure proper mode-locking but can drift over time. In order to accommodate this drift, a feedback system has been designed to adjust the modulator bias automatically to stay at the optimum value without tuning by the users. An RF spectrum is shown in Figure 1-3. The signal/noise ratio is well above 70 dB. Jitter studies using an Agilent E5052B signal source analyzer resolve a phase noise less than 200 fs integrated from 1 Hz to 10 MHz.

Figure 1-2. Fiber based seed laser system.

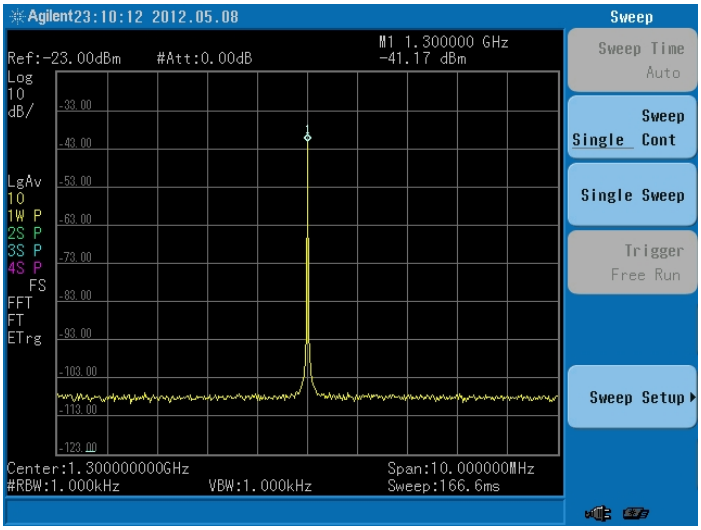

Figure 1-3. RF spectrum of the seed laser locked at 1.3 GHz.

The fiber oscillator pulses are sent through a pulse picker (Calmar model EPG-01FML12), in which a 81.25 MHz pulse train is selected from the 1.3 GHz pulse input. The output is amplified in 2 stages to reach 5 nJ per pulse. The standard deviation of the laser phase is 212 fs during a 10 hour span without noticeable drift, which is much better compared to the same measurement with a similar setup on the GE-100 manufactured by Time-bandwidth Inc. or the Tsunami Laser system manufactured by Spectra-physics.

The output from the seed laser then goes through a second pulse picker unit (Con-optics) and is reduced to a 3 MHz train as required at FAST. This pulse train can be up to 1 ms long. The extinguishing ratio through the pulse picker is more than 120:1, and the pulse-pulse amplitude fluctuations are less than 3%.

1.2 RF Gun

The RF photocathode electron gun is identical to the guns developed at DESY Zeuthen (PITZ) for the FLASH facility. As mentioned earlier, it is a normal-conducting 1½ cell 1.3 GHz gun operated in $TM_{010,\pi}$ mode, with a Q_L of ~11,700, and driven by a 5 MW klystron. The power is coupled into the gun via a coaxial RF coupler at the downstream end of the gun. The gun is capable of average DC power dissipation of ~20 kW and requires a dedicated cooling water skid. A temperature feedback system will regulate cooling water temperature to better than ±0.02 °C for good phase stability. The gun

will be routinely operated at peak gradients of 40-45 MV/m, and output beam kinetic energy of ~5 MeV. The peak gradient is given by

$$E[\frac{MV}{m}] = 23.6\sqrt{P[MW]},$$

where P is the measured power at the cavity.

The photocathode is a 10 mm diameter polished molybdenum disk coated with Cs_2Te with 5 mm diameter photosensitive area. It is illuminated by 263 nm wavelength laser light which is directed onto the photocathode by a 45° off-axis mirror located downstream of the RF coupler.

The photocathodes are coated at a separate facility on the Fermilab site, transported under vacuum to the photocathode transfer chamber mounted on the upstream end of the gun, and inserted into the upstream end of the gun via external manipulators, all under vacuum. Several photocathodes have already been prepared and their quantum efficiency measured to be ~10% when new. The photocathode preparation, transport, and transfer chambers were developed and built by D. Sertore at INFN Milano and commissioned at Fermilab.

For emittance compensation the gun is surrounded by 2 solenoid magnets built by DANFYSIK, each powered by a 500 A power supply also built by DANFYSIK. Each magnet has a peak field of 0.28 T at 500 A. Normally the magnet currents are set so the field at the photocathode is 0 kG in order to minimize beam emittance, however the field can be set to > 1 kG at the photocathode for the production of angular-momentum dominated beams and flat beam production. Each solenoid can be moved transversally to center the magnetic field on the beam axis, and in addition the downstream solenoid can be moved longitudinally to further optimize the magnetic field shape. ASTRA simulations indicate that transverse normalized emittances of 4 μm can be attained at a bunch charge of 3.2 nC, laser pulse length of 3.2 ps RMS, and peak gun electric field gradient of 40 MV/m. Stretching the laser pulse length will produce slightly smaller transverse beam emittance out of the gun, as will higher gun gradients.

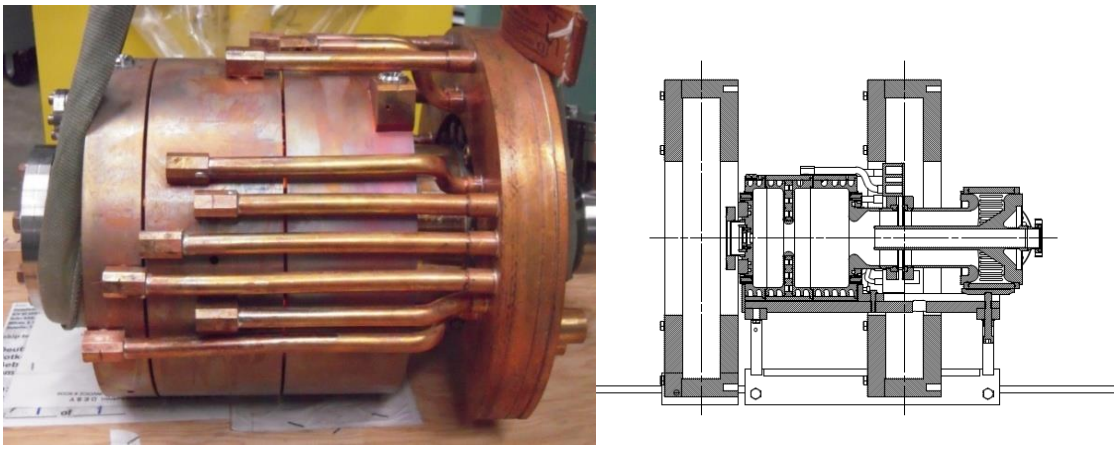

Figure 1-4. Left image is of the RF gun cavity prior to installation. The right image is a cut-away view of the RF gun cavity, solenoid magnets, and ceramic RF resonator.

1.2.1 RF Gun Cavity Water System

The RF power to the gun is supplied by a 5 MW, 1.3 GHz klystron. The temperature control loop stabilizes the temperature of the RF Gun when RF power is applied and, also, during no RF power cycles. The temperature control loop regulates the water temperature to ±0.18 ºC which, at a center frequency of 1.3GHz, keeps the frequency shift of the Gun within 5 kHz (23 kHz/ºC). A 5 kHz shift corresponds to a reflected power less than –22dB.

The task of the cooling system is to mix the outgoing warm water with the supply LCW water regulating the desired temperature of the circulating water. The cooling skid is located outside the radiation shielding and water is pumped through approximately 80 feet of piping. A PLC is integrated into the cooling skid to read back the temperature and flow measured by the different sensors and to control the flow rate of the LCW. The temperature of the LCW supply is stabilized to 90±1 ºF (~32.22 ±0.5 ºC) by an external control system running on an independent PLC. The amount of the incoming supply LCW is controlled by a fine pneumatic valve that allows a flow rate between 0 and 15 GPM. The position of the valve is controlled by a dedicated PID loop built into the valve controller. A heater is used to mix the LCW cold water and the warm water from the RF Gun and can supply between 0 and 12 kW of power. The mixed water flows to the gun at a fixed rate of 15 GPM through nine cooling channels, seven with 10mm ID and two with 6 mm ID tubing connections, cooling down the cavity. The

return water from the gun is split between the heater and a return connection to the main LCW chiller system.

1.2.2 Diagnostic Table

A diagnostic table is immediately downstream of the RF Gun. Figure 1-5 shows the layout of the FAST Front-End. The table contains 2 beam instrumentation crosses (a 9-way cross and a 6-way cross), 2 horizontal and vertical trim dipole magnets, 2 cameras with associated lens tube hardware, 2 sets of horizontal and vertical beam position monitors (BPM), two 100 liter/s ion pumps, a Laser Injection Light Box, and a Berghoz-style toroid.

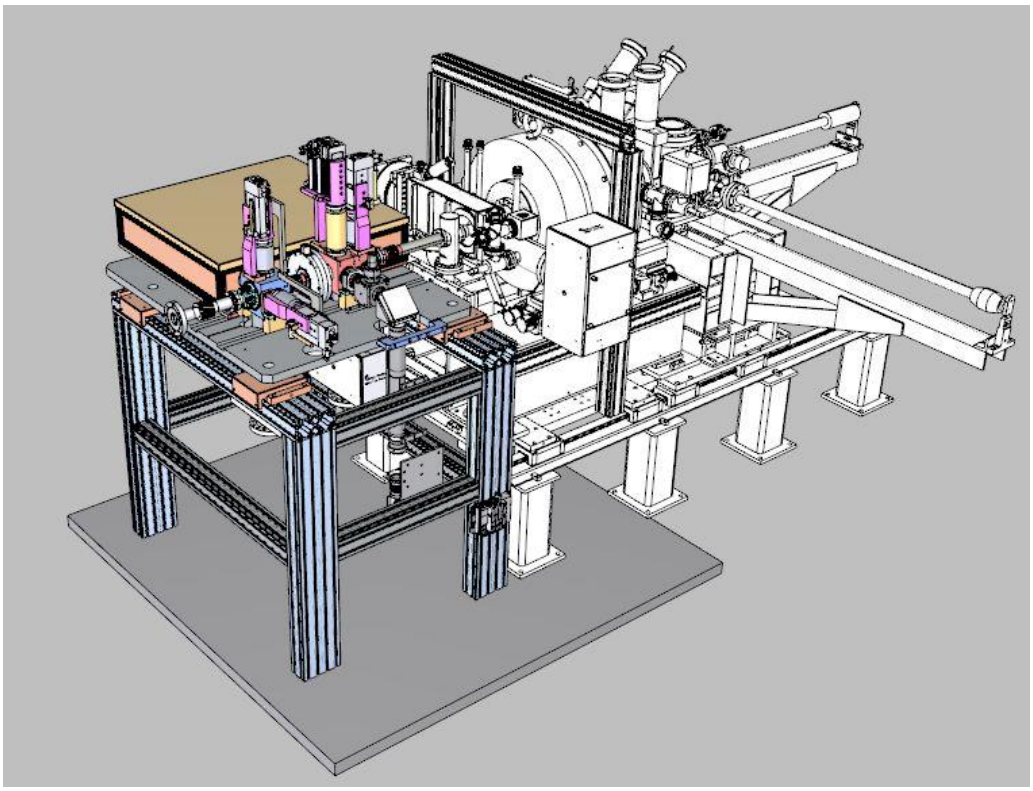

Figure 1-5. 3D model of the FAST Front-End. The Diagnostic Table is shown with color.

The 9-way Cross provides many functions. The upstream east viewport has an anti-reflection (AR) coated fused-silica window to allow the 264 nm UV laser to enter the vacuum system and reflect off a polished aluminum mirror, directing it to the photocathode inside the RF Gun. A mirror can be inserted via an actuator to direct scattered UV out of the vacuum cross and to a CCD camera attached to the upstream west side AR coated fused-silica window. This will provide a picture of the photocathode surface. A double actuator is mounted on the downstream end of the cross and moves a dual position holder contained in the edge-welded bellows. The first position inserted into the cross is the target, a piece of fused-silica glass 19 mm in diameter with concentric circles 1 mm apart. An LED inside the lens tube, affixed to the downstream west side of the cross, illuminates the target and allows the focus to be set on the networked camera connected to the lens tube. The next position in the holder is the 25.4 mm diameter cerium doped YAG crystal. Since the target and the crystal are in the same plane, the camera does not require any re-adjustment. Photoelectrons deposit their energy into the crystal, causing it to scintillate. The light is reflected to the CCD camera where the spot size is measured and transverse dimensions of the electron beam are calculated. A 3D CAD representation of the 9-way Cross is shown in Figure 1-6.

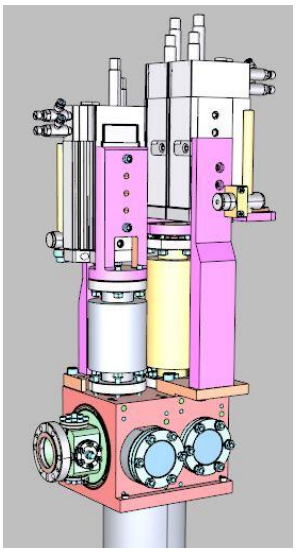

Figure 1-6. 3D CAD model of 9-way Cross.

The 6-way Cross contains one vertically mounted actuator and one horizontally mounted actuator. The vertical actuator inserts an electron beam collimator, a piece of copper with a 10 mm diameter hole through it. This will be used to collimate the electron beam if the dark current is too large and inducing quenches downstream. The horizontal actuator is used for inserting a Faraday Cup into the beam path. Only one device can be inserted at a time since the collimator and Faraday Cup operate at the same z-position. Collision bars are affixed to the actuators in the event an "in" command is issued to both. Figure 1-7 illustrates the layout of the 6-way Cross.

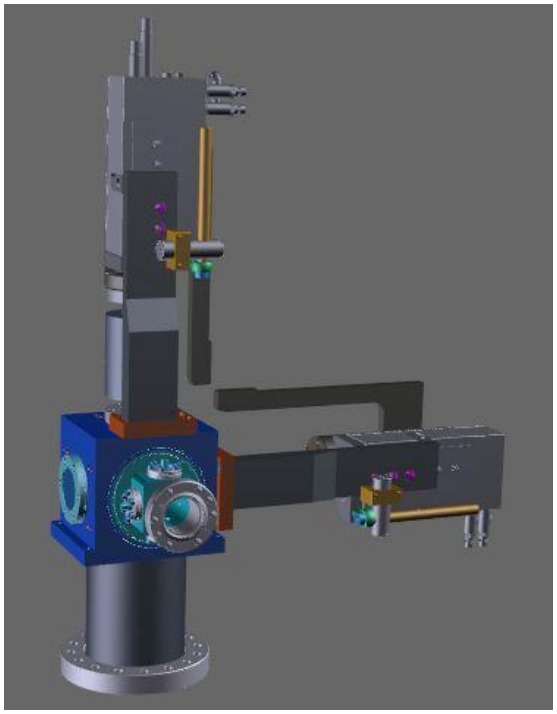

Figure 1-7. 3D CAD model of 6-way Cross.

Two sets of horizontal and vertical 5V, 10A corrector trim dipole magnets are attached to the upstream spool piece. These trims allow for the horizontal and vertical steering of the photoelectron beam through the crosses.

Each cross has a housing for horizontal and vertical button BPMs. The BPMs are located on the upstream side of the 9-way Cross and on the downstream side of the 6-way Cross.

There is one 100 liter/s ion pump connected to each cross. They are located under the table. The 6-way Cross ion pump also contains the interlocked vacuum switch for the UV laser safety system, convection and cold cathode gauges, and a turbo pump out port.

Because FAST uses Superconducting RF cavities for electron beam acceleration downstream of the Front-End, all components connected to the ultra-high vacuum system are required to be cleaned, assembled, and installed in cleanrooms using particle-free techniques. Once each cross assembly was completed, 2.75" blank flanges were installed on the upstream and downstream beam tubes. The assemblies were then vacuum leak checked with helium.

9-way Cross

The 9-way Cross is constructed entirely from 316L stainless steel. The BPM housing and inner sleeve were welded to the cross. The vacuum port flange is a 6" conflat (CF) and the BPM flanges are 1.33" mini-CF. All other flanges are 2.75" CF.

The heavily machined crosses contain several blind threaded holes. Fastener hardware for the crosses is all metric and made of titanium type 2 rolled threads or silicon-bronze.

Cathode Viewing Mirror Assembly

The Cathode Viewing Mirror assembly is comprised of a 25 mm diameter X 4 mm thick aluminum mirror, mirror holder, actuator-flange, actuator, fused-silica window, 50 mm travel edge-welded bellows, lens tube, and CCD camera. Figure 1-8 shows the 3D model of the Cathode Viewing Mirror assembly.

When an image of the photocathode is needed, the Cathode Viewing Mirror can be inserted into the 9-way Cross via a pneumatic actuator on the cross. Care must be taken, the RF Gun pulse will not be inhibited by the Machine Protection System (MPS)

if to the mirror is inserted into the beam path. Scattered UV light from the photocathode is directed out of the 9-way Cross and to a 5 megapixel networked GigE camera, sensitive to UV wavelengths, for inspection.

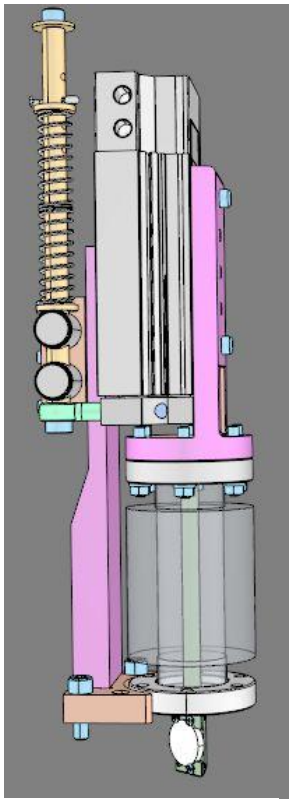

Figure 1-8. 3D CAD model of the Cathode Viewing Mirror assembly.

The holder is machined from 316L round stock and the fastening hardware is titanium screws. The screws used for connecting the holder to the actuator-flange are vented, as required, so as not to trap any gas in the vacuum system. The actuator-flange is also made from 316L round stock and is fastened to the actuator.

The mirror face has a 25 mm diameter aluminum coating on a 4 mm thick substrate of fused-silica. The mirror surface is enhanced to efficiently reflect UV. Three screws hold the mirror in place on the holder.

The Cathode Viewing Mirror assembly is vertically mounted to the upstream end of the 9-way Cross with six titanium studs and silicon-bronze nuts. A specially coated fused-silica window, identical to the Laser-In mirror window, is located at the upstream west side of the cross. The window is connected with similar hardware as the Cathode Viewing Mirror assembly. A 3" lens tube with an internal O-ring 1/8" thick is placed over the window. The O-ring makes a light tight seal around the window flange. The lens tube has a c-mount adapter attached to it for connecting the CCD camera.

Target and YAG Assembly

The Target and YAG assembly consists of a 19 mm diameter x 1.5 mm thick fused-silica glass reticle with concentric circles 1 mm apart and a line thickness of 25 μm wide, a 20 mm diameter mirror, a 25.4 mm diameter cerium doped YAG crystal 100 microns thick, 25 mm diameter mirror, a device holder, an actuator-flange, an actuator, a 100 mm travel edge-welded bellows, a CCD camera with attached lens tube, and a 2.75" fused-silica window. Layout of the Target and YAG assembly is seen in Figure 1-9.

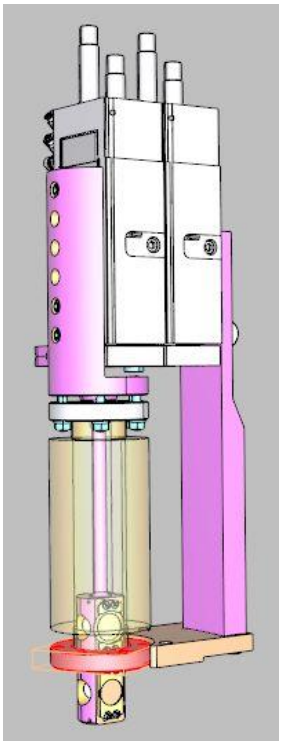

Figure 1-9. 3D CAD model of Target and YAG assembly.

The device holder is machined from 316L stainless steel round stock. A bracket holds the mirrors in place. Collars secure the Target and YAG to

the device holder. The fastening hardware is titanium button head screws. The holder connects to the actuator-flange with 3 vented titanium screws. The actuator-flange is also made from 316L round stock and is fastened to the actuator with cap screws.

The Target and YAG assembly is vertically mounted to the downstream end of the 9-way Cross with six titanium studs and silicon-bronze nuts. A 2.75" fused-silica window is connected to the downstream west side of the cross. A 1/8" thick O-ring is placed over the window flange to provide a light tight seal to the optics tube arm. A 5 megapixel GigE camera is connected to the end of the optics arm.

6-way Cross

Just like the 9-way Cross, the 6-way Cross is constructed entirely from 316L stainless steel. The BPM housing and inner sleeve are located on the downstream end of the cross. The vacuum pumping port flange is a 6" CF and the BPM flanges are 1.33" mini-CF while all other flanges are 2.75" CF.

Fastener hardware for the cross is all metric and titanium type 2 rolled threads or silicon-bronze. Actuator assemblies are connected to the cross with silicon-bronze socket head cap screws.

Faraday Cup Assembly

The Faraday Cup is constructed from oxygen-free high thermal conductivity (OFHC) copper with dimensions of 1"W x 1.75"H x 0.5"T. The Faraday Cup holder is machined from 316L stainless steel round stock. In order to isolate the Faraday Cup from ground, two ceramic stand-offs are connected between the holder and the cup. The Faraday Cup signal is directed out of the ultra-high vacuum system by means of a stainless steel wire with a diameter of 0.051". The wire is secured to the copper with a 316 stainless steel 4-40 thread ¼" length socket head cap screw. The formed wire is fastened to a copper-beryllium barrel connector. The opposing side of the connector is secured to the actuator-flange feed-through. Figure 1-10 shows the Faraday Cup during assembly in the cleanroom.

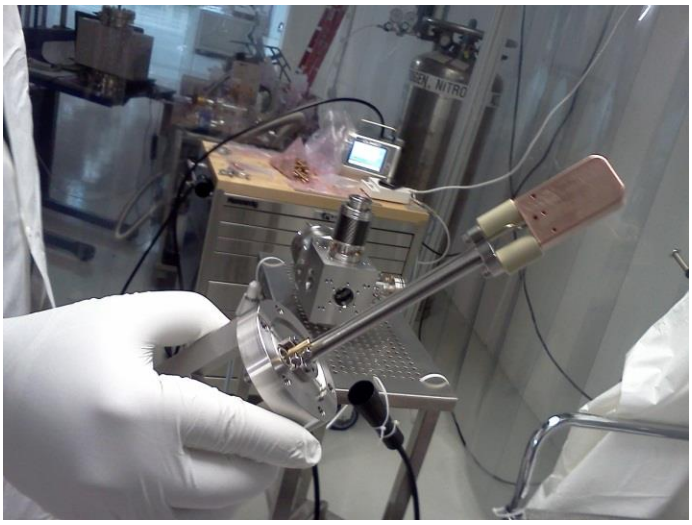

Figure 1-10. Faraday Cup assembly prior to attachment of the edge-welded bellows.

Collimator Assembly

The Collimator construction is identical to the Faraday Cup except that there is a 10 mm diameter hole through the OFHC copper. Assembly of the Collimator is, also, identical to that of the Faraday Cup. Figure 1-11 shows the Collimator assembly in the cleanroom.

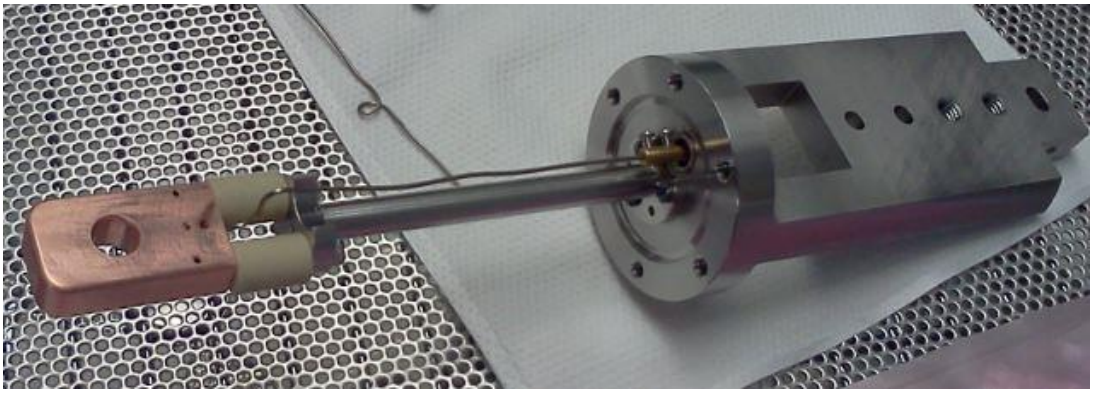

Figure 1-11. Collimator assembled in the cleanroom, less the edge-welded bellows.

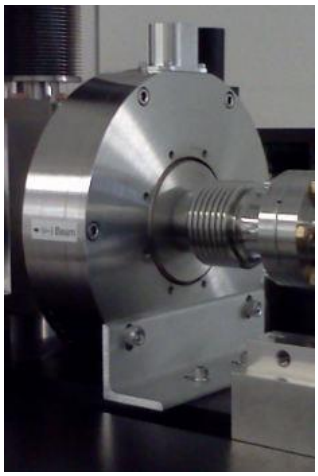

Figure 1-12. Berghoz style toroid installed on the Diagnostic table.

Berghoz-style Toroid

Information forthcoming.

Trim Dipole Magnets

Four trim dipole (pair) magnets are located on the upstream side of the Diagnostic Table. The magnets are comprised of copper wire wound around an iron core, which are then placed on a machined aluminum corrector coil magnet mount. The upstream pair of trim magnets, H100 and V100, are installed next to the downstream flange of the RF Gun vacuum gate valve. Magnets H101 and V101 are located on the 9-way Cross BPM flange. Figure 1-13 shows the trim magnets installed around the beam tube. The horizontal and vertical fields are independently adjusted with remotely controlled power supplies located outside of the Cave.

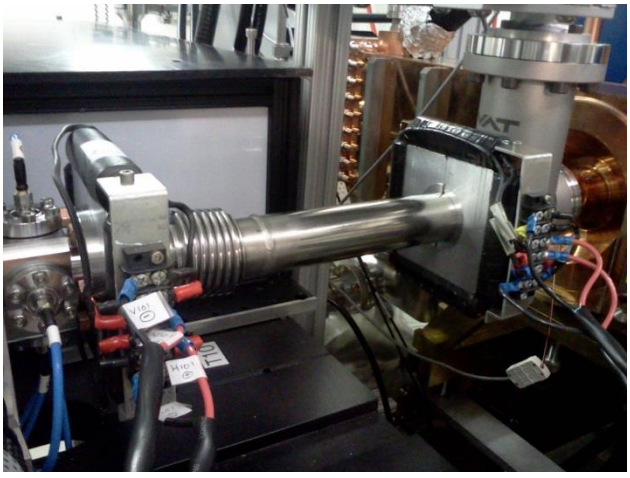

Figure 1-13. Trim dipole magnets installed on upstream side of Diagnostic table.

Beam Position Monitors

There are 2 horizontally and 2 vertically mounted button BPMs on each cross. The body of the BPM is a 1.33" mini-CF flange made of 316L stainless steel. The beam position pickup is 316L stainless steel, the electrical feed-through is constructed from molybdenum, and the electrical isolator is alumina. An SMA connector on the top of the flange has its gold-plated beryllium-copper center contact pin laser welded to the

molybdenum feedthrough. A copper canted coil spring keeps the flange grounded to the cross. Figure 1-14 shows the BPM pickup attached to the flange.

Figure 1-14. Button BPM prior to installation.

1.3 CC1, CC2, and the Low Energy Beamline

The injector beamline layout is shown in Figure 1-15. After a short instrumentation section, the electron gun is followed by two SRF cryomodules to accelerate beam up to 50 MeV. Each of these cryomodules contains a 9-cell L-band cavity operating at 1.3 GHz, driven by a 300 kW klystron, and capable of average accelerating gradients of >22 MV/m. These cavities can also be used to "chirp" the beam, ie., generate a time-momentum correlation, in preparation for bunch compression in the chicane. Downstream of these cavities is space allotted for a future SRF 3.9 GHz cavity intended to be used for bunch linearization during bunch compression.

The SRF cavities are followed by a quadrupole doublet to control the beam size for the emittance measurement, a matching section into the chicane, a 4-dipole chicane for bunch compression (R_{56}= -0.18 m), and a matching section into the vertically downward-bending dipole to the low energy beam dump. The 22.5° dipole upstream of the dump will serve as the low energy spectrometer. There is beamline space allocated upstream of this dipole for the future installation of a 3.9 GHz deflecting mode cavity to be used for longitudinal phase space diagnostics. The low energy beam dump is capable of absorbing up to 400 W of beam power.

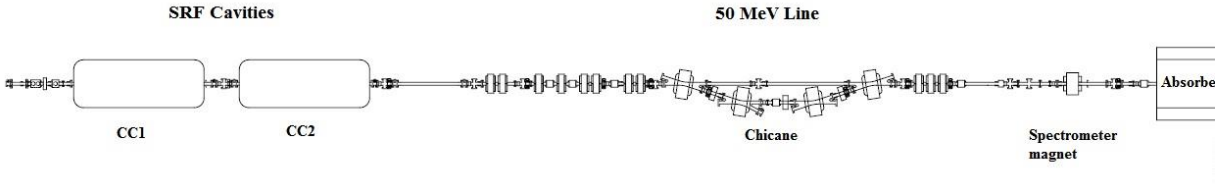

Figure 1-15. Low Energy Beamline layout.

There are 3 different types of magnets for the 50 MeV line (in addition to the gun solenoids): low energy correctors, quadrupoles, and dipoles. All magnets are bolted in 2 halves for possible removal or installation without breaking beamtube vacuum. All magnets can accommodate 2" O.D. 316L stainless steel vacuum tube.

1.3.1 Low energy dipole correctors

The low energy corrector magnets are air-cooled and were fabricated by Radiabeam Technologies, Inc. Each magnet has both horizontal and vertical corrector coils, and the magnet was designed to bolt around 3 3/8" conflat flanges. The maximum integrated field is 12.5 G-m at 7.6 A, which gives a beam kick of 7.5 mrad for 50 MeV beam. See Figure 1-16 for a magnet CAD representation.

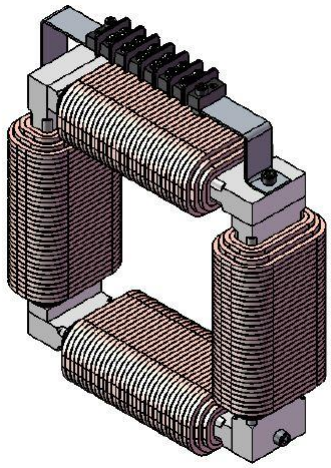

Figure 1-16. Low energy dipole corrector from 3D model.

1.3.2 Low energy quadrupoles

The low energy quadrupoles are air-cooled and were fabricated by Radiabeam Technologies, Inc. The maximum integrated field is 1.1 T at 9.0 A, which gives a focusing strength (K x L) of 6.6 G-m for 50 MeV beam. The effective magnet length is 0.167 m. See Figure 1-17 for a cross section. In addition, 3 smaller quadrupoles from

the A0 photoinjector, of a similar design, will be used in the injector chicane. Skew quadrupoles are identical and are simply mounted at 45° from normal quadrupoles.

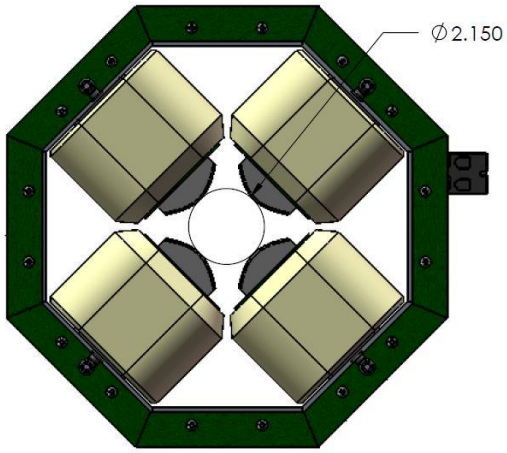

Figure 1-17. Downstream view of a low energy quadrupole.

1.3.3 Low energy dipoles

The low energy dipoles are air-cooled and were fabricated by Everson Tesla Corp. The maximum integrated field is 665 G-m at 8.0 A, which gives a beam kick of 23.5 deg for 50 MeV electrons. The effective magnet length is 0.300 m. See Figure 1-18 for a cross section. The clear aperture in the kick direction is >24 cm. The dipole will be rotated 90° about the beam axis to generate the 22.5° downward kick for the low energy beam absorber line.

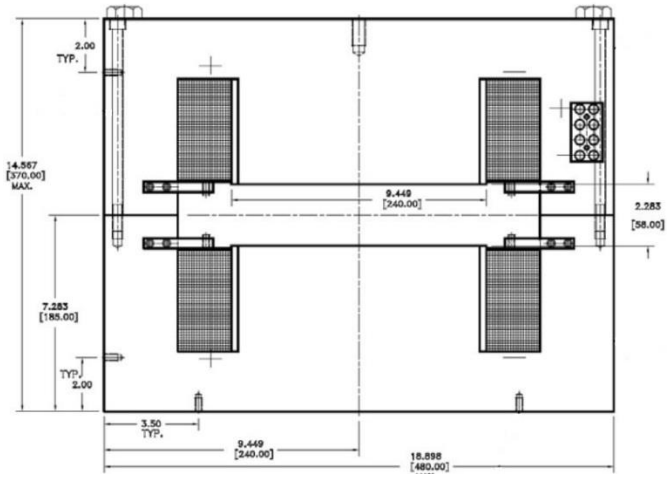

Figure 1-18. Low energy dipole magnet cross section.

The Low Energy Beamline installation (less CC1) and checkout was completed in March of 2015 and 20 MeV electrons were established to the absorber shortly thereafter. CC1 installation occurred in 2016 and 50 MeV commissioning of electrons to the low energy absorber was completed by June of that year. Figure 1-19 shows a portion of the installed beamline.

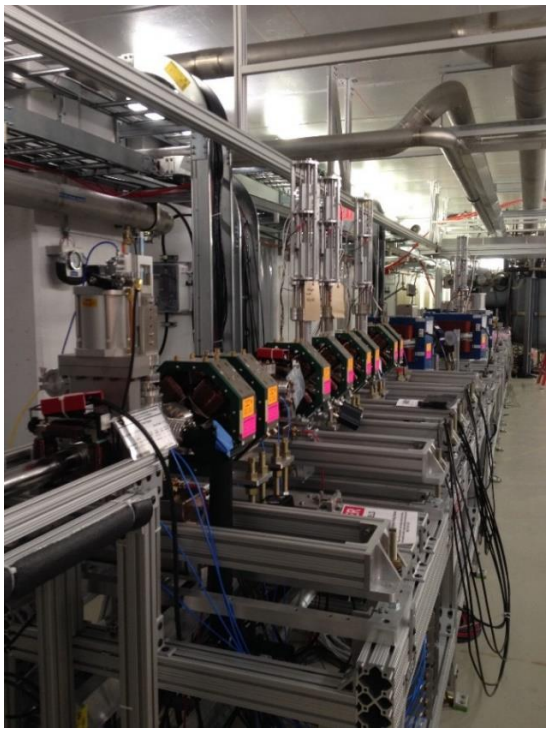

Figure 1-19. The Low Energy Beamline from downstream CC2. Note that all low energy magnet types are viewable in the picture.

1.4 Cryomodule CM2

Fermilab's second 1.3 GHz cryomodule (aka CM2 or RFCA002) was assembled between July 2011 and March 2012. During the installation of this module in the NML FAST Cave, a vacuum leak was discovered in the 2-phase helium circuit. The module was sent back to Technical Division (TD) in June 2012 and was partially disassembled to find the location of the leak and to repair it. The module was then reassembled and transported to NML in April 2013.

All eight cavities manufactured by industrial vendors were specifically selected on their likeliness to achieve the ILC design goal[1] based on their performance in individual RF tests. The cavities were first tested "bare" in a vertical liquid helium dewar using low-power continuous-wave RF. Cavities which met the ILC vertical test specification ($E_{acc} \geq 35$ MV/m, $Q_0 \geq 0.8 \times 10^{10}$) were then welded into individual helium jackets at TD and outfitted with a high-power input coupler. The high-power couplers were purchased from CPI. The couplers were cleaned and high power conditioned at SLAC. These "dressed" cavities were then tested in the Horizontal Test Stand using high-power pulsed RF. Qualified cavities along with a corrector coil magnet outfitted with an XFEL style helium jacket and a button style beam position monitor (BPM) were all assembled into a cavity string in the Cryomodule Assembly Facility (CAF) cleanroom at building MP9. Blade tuners were purchased from Incodema. The tuner motors and gears were purchased from Phytron and Harmonic Drive Inc. The magnetic shielding parts were designed by Fermilab and were purchased from Amuneal. The vacuum vessel, gas return helium pipe (GRHP) assembly and cold mass support posts were procured from Zanon in Italy.

The assembly of the cavity string was done in the CAF cleanroom. Eight qualified cavities, a magnet, a BPM and two gate valves were interconnected using bellows in the Class 10 cleanroom. The assembly of the cavity string is the most important step throughout the cryomodule assembly to ensure that the measured gradient of the qualified cavities is preserved. Particulate-free-flange-assembly techniques were

[1] The basic accelerating unit for the ILC is an SRF cryomodule that houses eight or nine 9-cell 1.3 GHz niobium cavities. The cavities are required to operate with an accelerating gradient of 31.5 MV/m and have an unloaded quality factor of $Q_0 \geq 1 \times 10^{10}$.

developed. The CM2 cavity string was assembled while following strict adherence to the CAF cleanroom working protocols.

After the string assembly was completed, the string was rolled out of the cleanroom into the cold mass assembly area at CAF using the assembly rail. The 2-phase pipes of the cavities were interconnected using titanium (Ti) bellows welded using an automated orbital welding machine. The cavities were then outfitted with magnetic shielding and blade tuner components. The cavity string was then lifted from the assembly fixtures and connected to the GRHP assembly forming the cold mass assembly. The cold mass assembly was then transported to Industrial Center Building (ICB). The X-Y axis alignment of the cavities to 250 microns was done using a laser tracker instrument. The cold mass was then transferred to the cantilever fixture for the welding of heat shields and multi-layer insulation (MLI). The cold mass was then moved to the final assembly area where the warm end high-power couplers and waveguides were assembled.

Throughout the cold mass assembly, several temperature sensors were installed on the critical components; RF measurements of the cavities were done several times and various vacuum leaks and pressure tests were conducted. After the final quality assurance checks, the fully assembled cryomodule was transported to the NML test area.

A single 1.3 GHz 5 MW klystron drives all of the cavities by means of variable tap-offs in a waveguide distribution system. Each cavity proved to operate at greater than 35 MV/m when tested in horizontal and vertical test stands. CM2, was installed in April 2013 and 2 K operation began November 2013. Figure 1-20 shows CM2 inside the Cave with the waveguide distribution system attached.

Figure 1-20. CM2 with waveguide distribution attached.

A testing procedure was developed from a previously installed ILC-type cryomodule, known as CM1. The cavities were tested one at a time. The procedure is summarized as:

- Cooldown the cavity and tune it to 1.3 GHz
- Set the motorized input coupler to a nominal position that is centered around $Q_L=3.5x10^6$
- Calibrate the forward, reflected, and transmitted power signals by using a few kW of forward power
- Perform on-resonance cavity and coupler conditioning with pulse lengths ranging from 20 μs to 1.3 ms
- Recalibrate forward, reflected, and transmitted power signals with 100 kW of forward power
- Determine maximum operating gradient
- Implement the Lorentz force detuning compensation adaptive feed-forward system which keeps the cavity in resonance through the entire pulse
- Perform measurements of X-ray and dark current as a function of gradient
- Measure the dynamic heat load as a function of gradient in order to determine Q_0

Once all cavities were individually tested, the waveguide distribution system was connected to all of the cavity couplers and the output of the 5 MW klystron. All cavities were then simultaneously powered and the gradients were increased. As seen from Figure 1-21, all but one, cavity 6, were able to reach the administrative limit of 31.5 MV/m. Cavity 6 was detuned slightly and the modulator voltage was increased from 7.9 kV to 8.1 kV. On 10/03/2014, CM2 ran at an average accelerating gradient of 31.5 MV/m per cavity with an overall accelerating voltage of 252 MV.

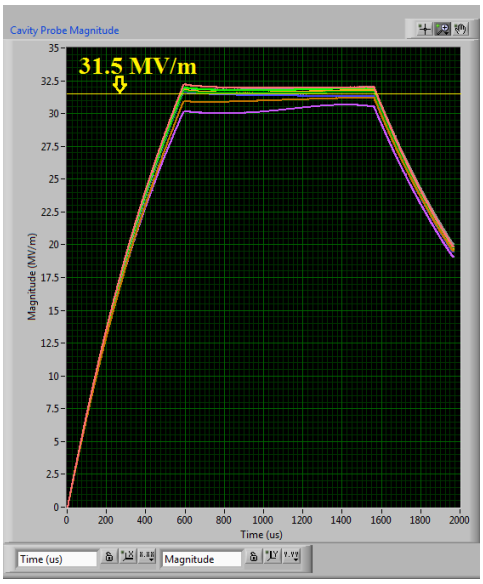

Figure 1-21. CM2 gradients for all cavities simultaneously.

1.5 High Energy Beamline

The High Energy Beamline begins when beam exits CM2[2]. The beamline consists of toroids, TPM stations, loss monitors, a fast-acting gate valve, quadrupoles, corrector trim dipoles, and large dipoles. Refer to Figure 1-22 for an image of the layout. The first large dipole (D600) will act as a spectrometer magnet to determine the electron beam's energy. The second large dipole (D604) will direct electrons either to the high energy beam absorber (HEA) or the Integrable Optics Test Accelerator (IOTA).

[2] Technically, the High Energy Beamline starts with the quadrupole triplet over the LEA. The triplet is used for focusing the beam into the cryomodule.

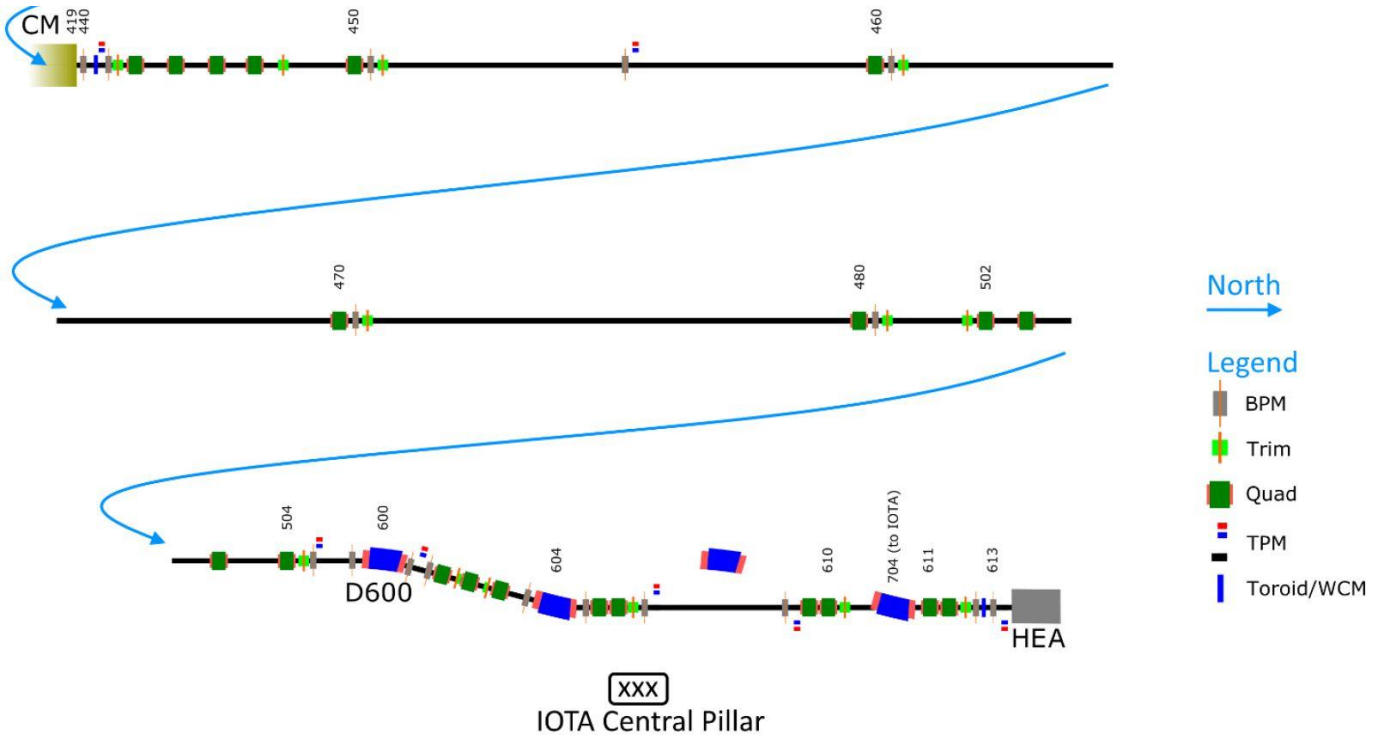

Figure 1-22. Layout of High Energy Beamline.

1.5.1 High energy dipole correctors

The high energy corrector magnets are air-cooled and were fabricated by Everson Tesla Corp. This magnet will serve as both horizontal and vertical corrector by rotating the magnet 90° about the beam axis for vertical correctors. The maximum integrated field is 200 G-m at 9.2 A, which gives a beam kick of 6.7 mrad for 900 MeV beam. See Figure 1-23 for a magnet cross section.

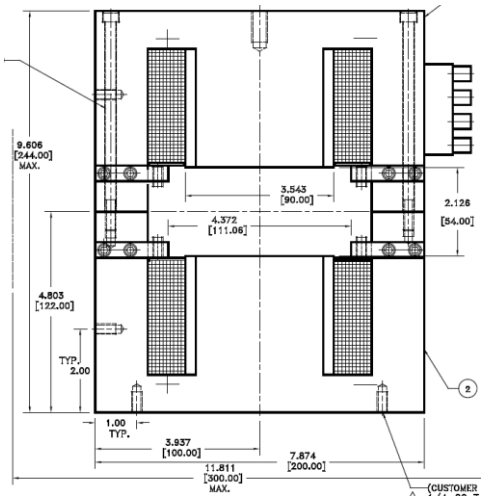

Figure 1-23. High energy corrector dipole cross section.

1.5.2 High energy quadrupoles

The high energy quadrupoles are water-cooled and were fabricated by Everson Tesla Corp. Water flow rate is 0.41 GPM (per magnet). The maximum integrated field is 8.3 T at 60 A, which gives a focusing strength (K x L) of 2.8 for 900 MeV beam. The effective magnet length is 0.417 m. Figure 1-24 shows a high energy quadrupole installed in the 300 MeV beamline.

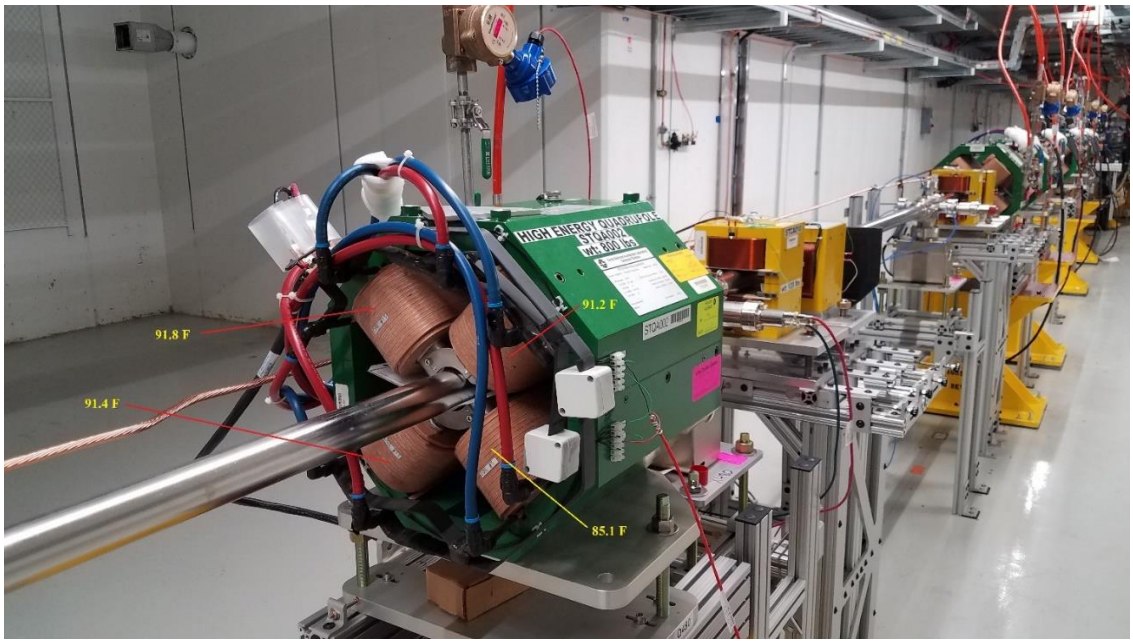

Figure 1-24. High energy quadrupole.

1.5.3 High energy dipoles

The high energy dipoles are fabricated from spare MI dipole laminations and spare MI dipole conductor. The laminated magnet cores were stacked by Fermilab, and the magnet was wound and assembled by Everson Tesla Corp. These magnets are water-cooled and take 7.5 GPM (per magnet). The maximum integrated field is 1.33 T-m at 1000 A, which gives a beam kick of 26.1° for 900 MeV beam. Effective magnet length is 1.277 m. See Figure 1-25 for a cross section. The clear aperture in the kick direction is 27.3 cm.

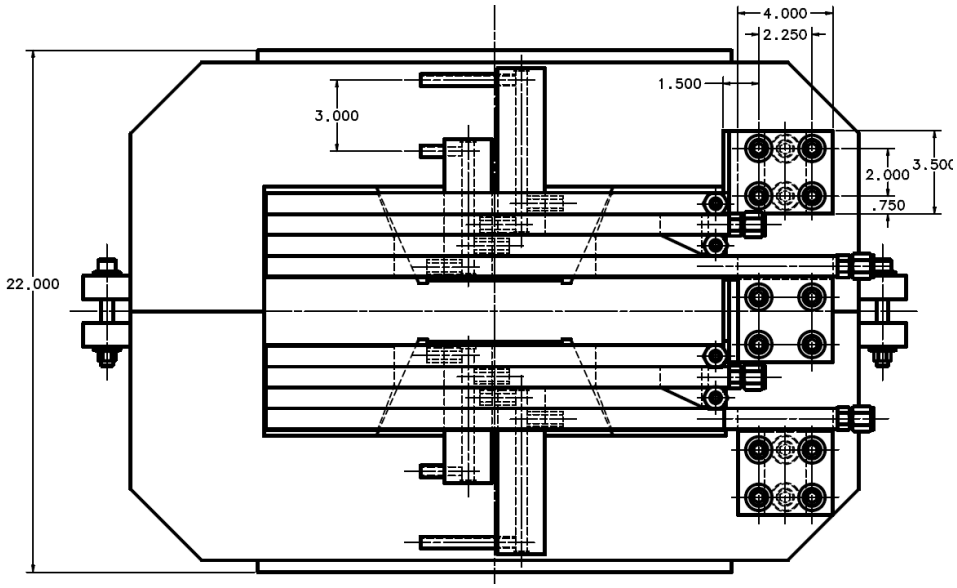

Figure 1-25. High energy dipole cross section.

1.5.4 Power supplies

Table 1-1 lists magnet power supply parameters. The 10 A and 60 A power supplies are similar in design to the standard FNAL Main Injector bulk power supplies and regulators. Currently, no 60 A power supplies are used at FAST since the design energy was reduced from 900 MeV to 300 MeV.

associated magnet	HE corr.	HE dipole	HE quad.
# installed magnets	29	4	29
total # PS (+15% spares)	33	5	33
int. field max. [G-m] or [T]	200.0	13300.0	8.3
magnet inductance [mH]	149	23	123
magnet resistance [ohms]	1.456	0.0116	0.317
magnet resistance (at max current) [ohms]	1.529	0.0122	0.333
Imax [A]	9.2	1000.0	60.0
Imax _full scale [A]	10.0	1000.0	60.0
polarity	bipolar	unipolar	bipolar
Vmax (@ Imax DC) [V]	14.1	12.2	19.0
minimum bits required	12	16	16
regulation [%]	0.200	0.010	0.010
ripple [%]	0.0200	0.0010	0.0010
bend at max. field spec. [mrad]	6.7 (900 MeV)		
bend at max. field spec. [deg]		26.1 (900 MeV)	
K x L at max. field spec.			2.8 (900 MeV)

Table 1-1. Magnet power supply parameters.

1.5.5 High Energy Absorber

The high energy beam absorber is located in an alcove at the end of the high energy tunnel (see Fig. 1-26). This alcove opens to a hatch at ground level just downstream of the electrical service building, through which the concrete shielding blocks were

stacked. The dump consists of two absorber cores each surrounded by 1.5 m thickness of steel, all encased in a 6.1 m x 6.2 m x 7.3 m stack of concrete. The absorber core consists of a stack of graphite disks, surrounded by a water cooled aluminum jacket, and backed by a copper plug. A dedicated, closed-loop, radioactive water skid (RAW) will provide the cooling water to the two high energy beam absorbers in series. In addition, the entire absorber core is encased in an inert gas (helium) to reduce oxidation of the graphite under the elevated temperature conditions.

A full energy deposition, thermal, stress, radiation damage, and lifetime analysis has been done on this beam absorber design using MARS and Finite Element Analyses with ANSYS. Based on these calculations, the beam dumps are designed to handle 80 kW of average beam power at energies up to 1500 MeV (full ILC intensity). The beam will be defocused by the final two quads in the beamline to a transverse spot size > 3 mm RMS in order to reduce the instantaneous peak energy deposition.

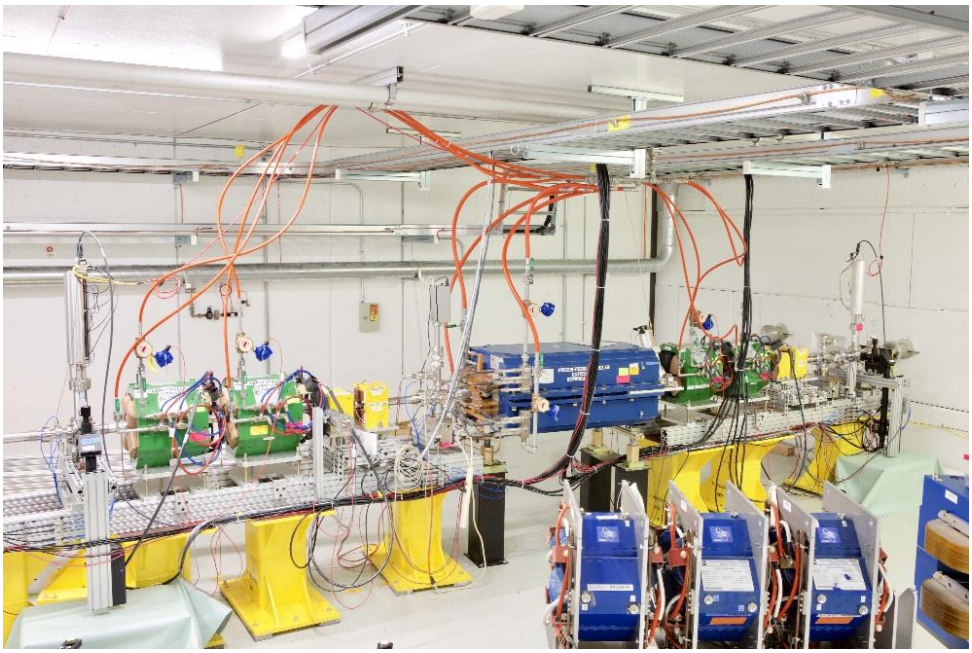

Figure 1-26 Downstream 300 MeV beamline. The HEA is located behind the concrete wall on the right.

1.6 The IOTA Ring

The Integrable Optics Test Accelerator (IOTA) is a storage ring for advanced beam physics research and is located at the downstream end of the 300 MeV beamline. It will operate with protons and electrons using injectors with momenta of 70 and 150 MeV/c,

respectively. The research program includes the study of nonlinear focusing integrable optical beam lattices based on special magnets and electron lenses, beam dynamics of space-charge effects and their compensation, optical stochastic cooling, and several other experiments.

1.6.1 IOTA Ring Design

The IOTA ring design is determined by the demands of the experimental program, limitations of the available space and cost optimization. The main requirements to the ring design are the following:

- capability of circulating either proton (up to 70 MeV/c momentum or 2.5 MeV kinetic energy) or electron (up to 150 MeV) beams;
- significantly large beam pipe aperture to accommodate large-amplitude oscillations of pencil beams and large size proton beam;
- significantly long straight sections to accommodate the experimental apparatus, including the nonlinear insert, and small enough footprint to fit in the existing FAST machine hall;
- significant flexibility of the optical lattice to accommodate all experimental options;
- precise control of the beam optics quality and stability;
- cost-effective solution based on conventional technology (magnets, RF).

The IOTA ring parameters are listed in Table 1-2 and its layout is depicted in Figure 1-27, where the major magnetic and diagnostic elements are shown.

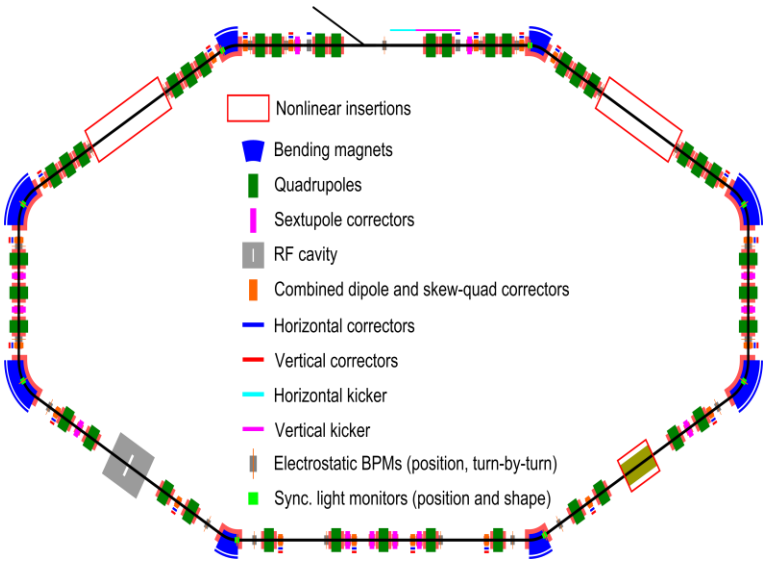

Figure 1-27. Layout of IOTA ring.

Nominal kinetic energy	e^-: 150 MeV, p+: 2.5 MeV
Nominal intensity	e^-: 1×10^9, p+: 1×10^{11}
Circumference	40 m
Bending dipole field	0.7 T
Beam pipe aperture	50 mm dia
Maximum b-function (x,y)	12, 5 m
Momentum compaction	-0.02 ÷ 0.1
Betatron tune (integer)	3 ÷ 5
Betatron tune chromaticity	-15 ÷ 0
Transverse emittance r.m.s.	e^-: 0.04 μm, p+: 2μm
SR damping time	0.6s (5×10^6 turns)
RF V,f,q	e^-: 1 kV, 30 MHz, 4
Synchrotron tune	e^-: 2×10^{-4} ÷ 5×10^{-4}
Bunch length, momentum spread	e^-: 12 cm, 1.4×10^{-4}
Beam lifetime	e^-: 1 hour, p+: 1 min

Table 1-2. IOTA Ring parameters.

The ring geometry is defined by 8 main bending dipole magnets (four 30-degree and four 60-degree bends) and 6 long and 2 short straight sections. The 2 short sections between 60-degree magnets, shown vertically in figure 1, are used for dispersion suppression and chromaticity correction. The top horizontal section is used for the beam injection. The lower-left diagonal section is occupied by the accelerating RF cavity. The remaining 4 long sections are designated for the installation of experimental apparatus, such as the nonlinear inserts for integrable optics, the electron lens, and optical stochastic cooling. The ring circumference is 40 m. The nominal bending magnetic field of 0.7 T allows for the maximum electron beam energy of 150 MeV. The 2.5 MeV kinetic energy of the proton beam from the proton injector corresponds to the momentum of 70 MeV/c and requires half the nominal bending field.

Focusing is provided by 39 quadrupole magnets. The correction system consists of 20 combined-function trim dipole (horizontal and vertical) and skew-quadrupole corrector magnets, 8 horizontal orbit correction coils incorporated in the main dipoles, 2 vertical bump correctors in the injection straight section, and 10 sextupoles for chromaticity correction. The lattice is mirror-symmetrical with respect to the vertical center line,

allowing for a cost-efficient powering scheme with the 39 power supplies powering the main quadrupole magnets (twelve 250 A, twenty 120 A, and seven 70 A supplies). The main dipoles are powered in series with the injection Lambertson by a single power supply. All of the corrector elements are powered by individual bipolar 2 A/15 V supplies reused from the Tevatron Collider.

The vacuum chamber in the straight sections is made of 316L stainless steel tube with a 2-inch internal diameter. In bending magnets, the vacuum chamber is Aluminum of rectangular cross-section with dimensions of 50×50 mm. Vacuum at a level of 6×10^{-10} Torr or better is maintained with the use of combination NEG[3] and ion pumping at 35 locations around the ring and in the transfer line. The IOTA ring shares a common vacuum with the FAST injector, where the vacuum specification is 1.5×10^{-8} Torr, and thus the transfer line will employ three 150 L/s combination NEG/ion pumps for differential pumping. The system is bakeable in situ up to 120 °C prior to use and each time the vacuum system is opened for modifications or maintenance. The high quality of the vacuum system is necessary for proton beam operation and the vacuum of 6×10^{-10} Torr determines the beam lifetime of 5 min for 2.5 MeV protons. The requirements for electron beam operation are much more relaxed, and a level of 3×10^{-8} Torr is sufficient for a beam lifetime of 30 min of 150 MeV electrons. The IOTA vacuum system is UHV and not required to be particle-free unlike the majority of the FAST Linac.

The injection system (located in the upper straight section in figure 1) consists of a Lambertson magnet and an adjacent stripline kicker. The horizontal 30°-bend Lambertron magnet delivers injected beam at a 1° vertical angle 27 mm below the ring main plane. The beam is then kicked on to the central orbit with a 25-kV pulse of the 1 m long vertical kicker. The kicker pulse length is suitable for single-turn injection (120 ns revolution period for the electron beam). The injection scheme also requires the localized distortion of the closed orbit, which is achieved by the special vertical orbit (bump) correctors up- and downstream of the injection region.

---

[3] **Non evaporable getters** (NEG), based on the principle of metallic surface sorption of gas molecules, are mostly porous alloys or powder mixtures of Al, Zr, Ti, V and Fe. They help to establish and maintain vacuums by soaking up or bonding to gas molecules that remain within a partial vacuum. This is done through the use of materials that readily form stable compounds with active gases. They are important tools for improving the performance of many vacuum systems. Sintered onto the inner surface of high vacuum vessels, the NEG coating can be applied even to spaces that are narrow and hard to pump out, which makes it very popular in particle accelerators where this is an issue. The main sorption parameters of the kind of NEGs, like pumping speed and sorption capacity, have low limits. The temperature range is from 0 to 800 K under HV/UHV conditions. The NEG acts as a getter or getter pump that is able to reduce the pressure to less than 10^{-7} Pa.

The RF accelerating system is provided by a dual-frequency cavity located in the lower-left diagonal section of Figure 1. The two gaps of the cavity operate at the frequencies of 30 MHz and 2.18 MHz, which correspond to the fourth revolution harmonic for 150 MeV electrons and 2.5 MeV protons, respectively. The high frequency gap can provide up to 1 kV accelerating voltage, sufficient for bunching the 150 MeV electron beam and replenishing the synchrotron radiation losses. The ferrite-loaded cavity has the Q value of 100 and is driven by a 100 W solid-state amplifier. The cavity tuning is achieved with variable capacitors driven by stepping motors.

The large number of quadrupoles allows for the flexibility of optics tuning to address the needs of beam physics experiments. The current set of optics solutions includes the following options: a) integrable optics (IO) with one nonlinear insert; b) IO with octupole string insert; c) electron lens; d) McMillan electron lens; and e) optical stochastic cooling (OSC). The basic lattice requirements for these options come from the nonlinear integrable optics theory (see section 3) and include the specific betatron phase advance between the nonlinear insert sections and the zero dispersion in the nonlinear insert. The sampling of wide range nonlinearity requires kicking the probe beam to large betatron amplitudes. Coupled with the machine aperture limitation, this determines the limit on the maximum value of the beta-function. Lastly, the optical stochastic cooling experiment requires a transverse beam emittance of less than 0.1 μm (rms normalized). The betatron tune chromaticity correction scheme employs 12 sextupole magnets in 6 families that are properly spaced in betatron phase advance to minimize their effect on the dynamics in the different operational scenarios.

1.6.2 Magnets and Power Supplies

Dipoles

The main dipoles are curved C-dipoles that will be powered to 518 A in order to provide the 0.7 T field to circulate 150 MeV electrons. The current will be 259 A for 2.5 MeV protons. A 30° dipole, less the vacuum chamber, is shown in Figure 1-28. Each dipole is connected to the NML LCW system.

Figure 1-28. IOTA 30° C-dipole.

The dipoles are powered in series with a PEI 240 kW 600 A power supply named IBEND located in ESB. The ACNET parameter is N:IBEND. The power supply is tied into the FAST Cave electrical safety system. The power supply will also trip off if any of the klixons from each magnet (3 per magnet) open. The klixon summation chassis is located at ESB in rack 904. Magnet LCW flow and temperature are processed in the Rittal cabinet and a contact closure will open if the PLC detects the flow and/or temperature beyond the set operable limits. A differential pressure sensor is connected to the LCW supply and return behind the power supply. Other detectable faults can be seen in the front panel image of Figure 1-29. There are 2 power sources for the PEI. Control power is 120 V and 480 V is provided from a separate power panel.

Figure 1-29. Left, IBEND power supply. Top, IBEND klixon chassis in RR904. Bottom right, interlock display panel for IBEND.

Quadrupoles

There are 2 styles of quadrupoles in IOTA. The first are refurbished quadrupoles colloquially referred to as "Dubnas." See Figure 1-30. The second style were manufactured by RadiaBeam Technologies.

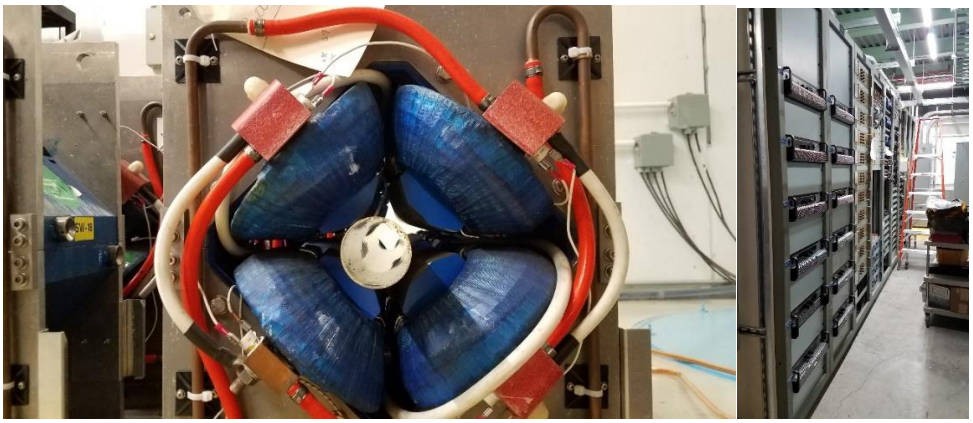

Figure 1-30. Refurbished Dubna quad prior to installation and quadrupole power supply racks in ESB.

Combined-function Magnets

The combined-function magnet has individually controlled coils that yield a skew quadrupole field along with horizontal and vertical trim fields. Each component of the combined-function magnet is controlled through an algorithm that determines the amount of current to send to each coil in order to create the field requested by the control room operator. A combined function magnet and it's associated power supply can be seen in Figure 1-31.

Figure 1-31. Combined-function magnet and associated ±2 A modified Recycler 16-channel power supply.

Sextupoles – Not installed at this time.

Octupoles – Installed. Documentation forthcoming.

Lambertson and Kickers

As mentioned prior, the horizontal 30°-bend Lambertson magnet delivers injected beam at a 1° vertical angle 27 mm below the ring main plane and is then kicked on to the central orbit with a 25-kV pulse of the 1 m long vertical kicker.

Beam enters the field region of the 18-turn coil Lambertson via a 1" diameter beamtube. The 0.7 T field is created via 18-turns of a 12x12 mm copper wire containing a 6 mm cooling channel hole. The "field-free" region utilizes a 2" diameter beamtube. The magnet also contains a 40-turn corrector coil for fine tuning the beam trajectory.

The kicker hardware and electronics reside in ESB, against the north and west walls. The kicker cable lengths are trimmed so the reflected pulse does not occur at a harmonic of the beam period. Figure 1-32 shows a 3D view of the Lambertson and vertical kicker.

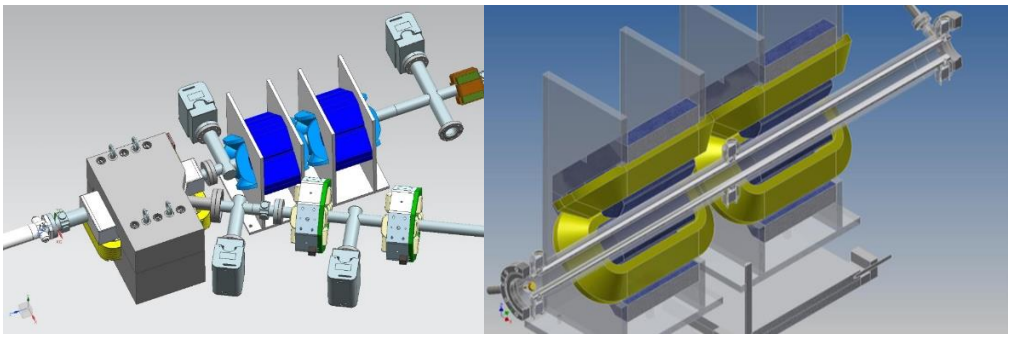

Figure 1-32. Left, Lambertson magnet with 1" diameter beamtube injection line. Right, vertical kicker with elliptical beamtube and nested inside 2 Dubna quads.

Nonlinear Insert

Figure 1-33. Nonlinear magnet under development at RadiaBeam Technologies.

Injection Dipole D604

Dipole D604 is fabricated from spare MI dipole laminations and spare MI dipole conductor. The laminated magnet cores were stacked by Fermilab, and the magnet was wound and assembled by Everson Tesla Corp. The magnet is water-cooled and takes 7.5 GPM (per magnet). The maximum integrated field is 1.33 T-m at 1000 A, which gives a beam kick of 26.1° for 900 MeV beam. Effective magnet length is 1.277 m. The clear aperture in the kick direction is 27.3 cm.

The D604 power supply is a Magna-Power Electronics identical to the D600 power supply. Both are located in RR968 in ESB. Since the proton source will be connected to the upstream east side vacuum port, there is a Spang switcher for swapping the polarity of the magnet leads so the positive charged beam can be injected into IOTA. Figure 1-34 shows the reversing switch front panel.

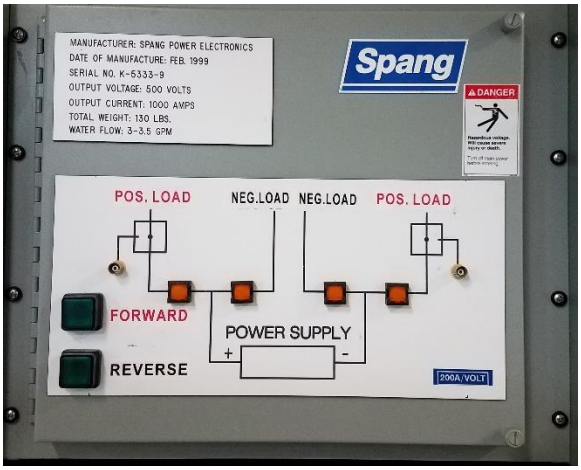

Figure 1-34. D604 power supply load reversing switch.

1.6.3 Transfer Line

The 150 MeV electrons are directed from the FAST injector toward the IOTA ring when the magnetic field in D604 is non-existent. The injection line consists of magnetic elements Q801, H801, V801, and Q802. After Q802, electrons enter the IOTA Lamberston field region and are injected into the ring. Magnets Q801 and Q802 are the same type as those found in the Low Energy Beamline. The two trim magnets are

the same style as used in the High Energy Beamline. A top view drawing of the injection line can be seen in Figure 1-35

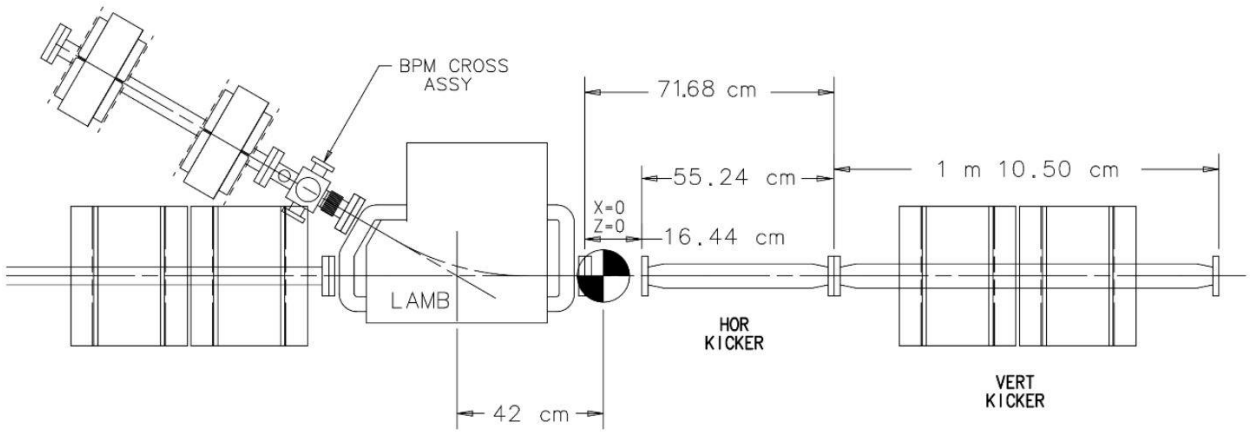

Figure 1-35. IOTA injection area diagram.

1.6.4 RF System

The difference in the periods of the electrons and protons presents a challenge for both the RF system and for instrumentation. The RF system will initially operate at harmonic h=4, or 30 MHz, for electrons. The nearest harmonic for protons would be 56; however, as shown in Figure 1-36, the planned voltage of the RF system is not nearly enough to fully bunch the proton beam at this frequency. For this reason, the RF system has been designed to also operate at 2.18 MHz, which corresponds to h=4 for protons. As shown in figure xx, this can fully bunch the proton beam at a reasonable voltage of 500 V.

The different RF frequency presents something of a challenge for the BPMs, which will initially be designed to operate at 30 MHz. One solution would be to bunch the beam at 2.18 MHz, but then modulate it with the 30 MHz RF to generate a signal in the BPMs. Unfortunately, our simulations show that the signal from such a modulated beam would only correspond to about 10% of the total protons, which would significantly degrade the position resolution. Another solution is to modify the BPMs electronics to work with both frequencies. Among other things, this would require

changing the input coupling to capacitive but modifying the Antiproton Source ARF4-2 cavity was the easiest and cheapest option.

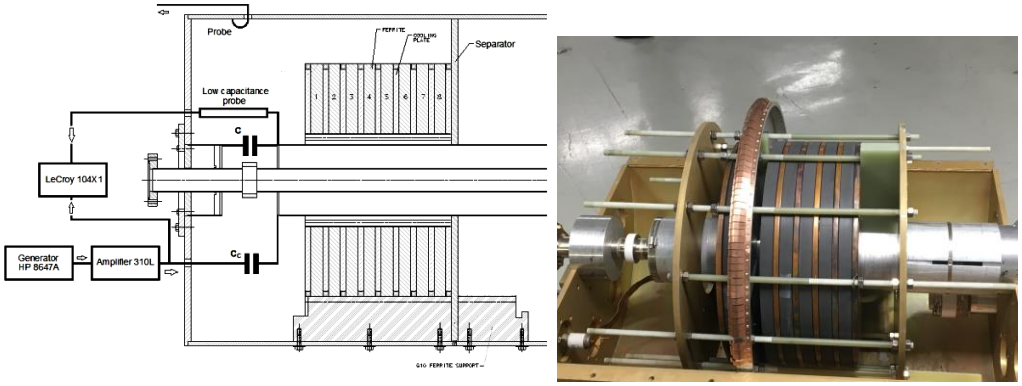

Figure 1-36. Left, RF cavity setup. Right, ARF4-2 refurbished with beamtube and ferrites installed.

1.6.5 Instrumentation

Transverse Profile Monitor

Profile measurements of electrons for the IOTA ring are provided by imaging of the synchrotron radiation emitted from the dipole magnets. The design of the beampipe dictates that the collected light originates from the entrance of the 30° magnets and from the center of the 60° magnets. The light is transported to a light-tight box positioned on top of the dipole containing a GigE-type CCD camera, see Figure 1-37. The optical trajectory is controlled by a remotely-moveable turning mirror and an iris which controls the length of the emission source seen by the camera. Focusing is done via a 400 mm focal length lens resulting in a magnification of 0.837.

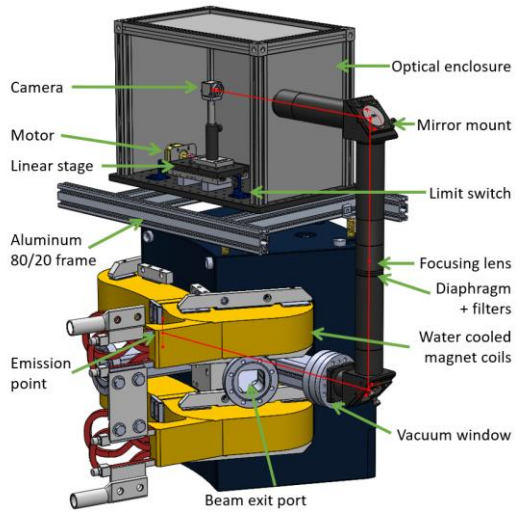

Figure 1-37. Synchrotron light transport system.

Beam Position Monitors

The beam position monitors (BPMs) in both the electron injector and the IOTA ring consist of 11-mm-diameter button electrodes with a subminiature type-A (SMA) feedthrough in a 47.5-mm inner-diameter housing. Each instance contains 4 buttons to provide both horizontal and vertical measurements. The IOTA ring contains 20 standard BPMs, plus one with a wider aperture near the injection point. There is in-tunnel signal conditioning, and out-of-tunnel downmix electronics for 650 MHz, with digital signal processing via custom 12-channel, 250-MS/s, VME/VXS digitizers. The system can provide position resolutions of <50 μm for a single 3-nC bunch, and ~1 micron for 3000 bunches. It provides both relative intensity and phase and is sensitive down to ~50 pC/bunch.

Wall Current Monitor and Toroid

Beam intensity measurements are made with toroids, and high-bandwidth wall current monitors (WCM). The WCM features a compact 50 mm width design, including flanges, and has a 48 mm diameter bore. The frequency response ranges from ~16 kHz, due to gap resistance and ferrite inductance, up to ~4 GHz limited by the microwave cutoff of high-order modes. The WCM and toroid provide bunch-by-bunch intensity via an analog integrator and custom digitizer. Dual channels are used to sample the signal and background for each bunch. A 3 nC bunch charge results in a 1% accuracy

in relative bunch intensity. The toroid is also a compact design and provides the absolute calibration for the WCM. There is one WCM and toroid for the IOTA ring.

Gas-Jet Profile Monitor - Under development

1.7 Experiments in FAST and IOTA

1.7.1 Inverse Compton Scattering

The electron beam energy in the IOTA/FAST beamline will be increased to 300 MeV when the accelerating cryomodule (CM) becomes operational. This will allow the generation of hard X-rays or gamma rays by scattering the electron beam off laser photons via the process generally called Inverse Compton Scattering (ICS). The electrons oscillate in the transverse electric fields of the laser pulse and emit radiation in the direction of their motion. For head-on collisions between the electron and laser beams, the energy of the photons emitted along the electron beam axis is related to the laser photon energy E_L as $E\gamma=4\gamma^2E_L$. Thus, a 1eV laser photon and a 300 MeV electron beam, can create ~1.5 MeV photons via the ICS process. High photon rates and spectral brilliance require the use of a high-power laser system. In the IOTA/FAST injector, the same IR laser system used to generate the electrons from the photocathode will be used to collide with the electron beam. The laser beam energy will in the first stage be increased from 50 μJ to about 50 mJ by two single pass amplifiers. In the second stage, a high finesse optical cavity will be used for amplification to raise the laser beam energy to the Joule level. The scheme is to trap each laser pulse in the cavity with low loss mirrors at each end and coherently combine several laser pulses before colliding them with an electron bunch in the cavity. Both laser and electron beams will have to be focused to small spot sizes at the collision point to increase the number of scattered photons produced while high brightness also requires a small electron bunch length. With typical FAST parameters, we expect to produce about 106 photons per electron bunch and a spectral brilliance of about 10^{20} photons/s-(mm-mrad)^2 — 0.1% BW and a photon energy spread of about 1% (figure 30). Design of the optical cavity with high amplification, while controlling position and angular misalignments within allowed limits, and synchronization of the colliding pulses will be the major issues. Progress in the construction and operation of a four-mirror optical cavity was recently

reported. A higher laser sampling rate above the present value of 3 MHz will also help in reducing the cavity length and will be explored as a possible option.

1.7.2 Optical Stochastic Cooling

Due to large longitudinal particle density, N/σ_s, the beam cooling times of few hours required for luminosity control in high energy hadron colliders cannot be achieved with traditional stochastic cooling technique in the microwave frequency range ($\sim 10^9$–10^{10} Hz). A practical scheme operating in the optical frequency range — optical stochastic cooling (OSC) — allows the increase of cooling bandwidth by a few orders of magnitude to about $\sim 10^{14}$ Hz. In OSC, a particle emits electro-magnetic radiation in the first (pickup) wiggler. Then, the radiation amplified in an optical amplifier (OA) makes a longitudinal kick to the same particle in the second (kicker) wiggler, as shown in Figure 1-38. A magnetic chicane is used to make space for the OA and to delay a particle so that to compensate for a delay of its radiation in the OA resulting in simultaneous arrival of the particle and its amplified radiation to the kicker wiggler. A particle passage through the chicane has a coordinate-dependent correction of particle longitudinal position which, consequently, results in a correction of relative particle momentum, $\delta p/p$, with amplitude ξ_0 so that:

$$\delta p/p = -\xi_0 \sin(k\Delta s).$$

Here $k=2\pi/\lambda$ is the radiation wave-number.

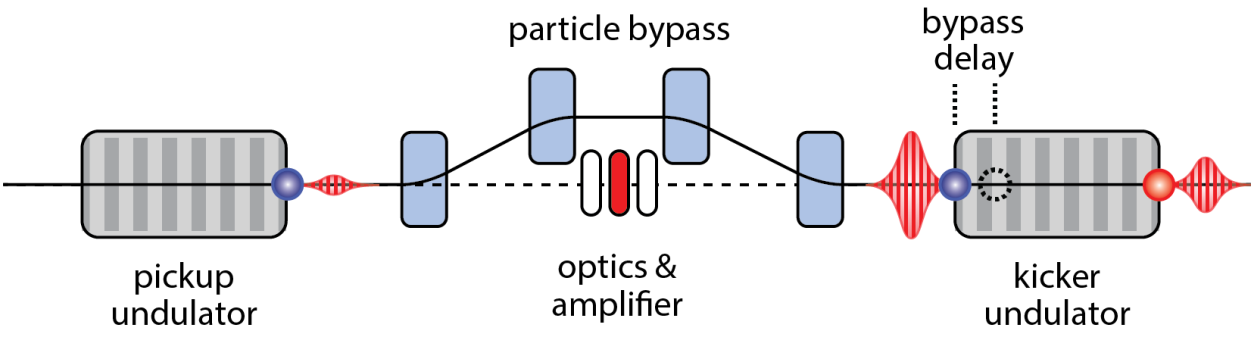

Figure 1-38. Layout of OSC.

SECTION 2

DESIGN AND LAYOUT OF THE PROTON INJECTOR

2.1 Proton Source

A proton source for the IOTA ring is being refurbished from the former High Intensity Neutrino Source (HINS). The proton source itself is a duo-plasmatron that feeds a radio frequency quadrupole (RFQ) before the 2.5 MeV proton (p+) beam passes through a debuncher cavity. The original HINS source included a number of other RF structures which will not be used, and the cooling problems that prevented the RFQ from reaching its originally specified duty factor will not be an issue for this application. Recommissioning of the 2.5 MeV p+ beam from the RFQ began in 2017. The beam will be characterized using an Allison Scanner, Faraday cup, and other instrumentation in situ at its current location, the Meson detector Building (MDB). This will allow the RFQ commissioning to progress independently from any construction or commissioning constraints with respect to the electron injector or the IOTA ring. Once the RFQ proton source commissioning is complete at MDB, components will be moved from MDB to the FAST facility at NML to be reassembled alongside the high energy beamline in the NML cave extension, with commissioning of the 2.5 MeV p+ beam into the IOTA ring in calendar year 2020.

2.2 Proton Injector

As described above, an electron beam will initially be used to probe the optics of the IOTA ring. However, because the space charge effects on the electron beam will be negligible, and space charge dominated proton beam will be used for most of the direct tests of the inherent stability. The IOTA proton injector will reuse the 70 MeV/c (2.5 MeV kinetic energy), low duty factor RFQ that was originally built and commissioned for Fermilab's High Intensity Neutrino Source (HINS) program. This program was terminated when a leak in the water cooling system prevented this RFQ from reaching its design 1% duty factor. In our application, it is planned to use the RFQ for 1.7 μsec pulse, at 1 Hz maximum repetition rate, so no water cooling of the RFQ will be needed.

The RFQ itself is a four-vane design, operating at 325 MHz. The source consists of a 50 kV filament proton source, capable of delivering 8 mA.

The dipole that is used to switch electrons between the IOTA ring and the HEA (D604) will also serve to switch protons into the ring. The 2.5 MeV energy of the protons corresponds to roughly half the nominal rigidity of the IOTA electron beam, but the velocity is only 0.073 c, which presents some challenges. We plan to inject protons in the same direction as the electrons, using the same Lambertson magnet and kicker. Obviously, this means all field polarities will have to be reversed, and the pulse length for the kicker will need to be selectable. The RFQ will be followed by a 325 MHz debunching cavity to reduce the momentum spread somewhat. Nevertheless, because of the low β of the proton beam, the momentum spread will cause the beam to completely debunch within the first turn or so, making the 325 MHz bunch structure irrelevant.

SECTION 3

ACCELERATOR CONTROL SYSTEMS

3.1 Controls

Like any accelerator at Fermilab the implementation of an SRF Electron Linac at NML requires a control system in order for the operator to monitor readbacks from and make appropriate changes to the various systems that comprise the facility. One might assume that the best control system would be one tailored to the machine and with the largest support base, but these are not so easily reconciled. Other accelerators at Fermilab rely on the Accelerator Controls Network (ACNET), a custom, in-house control system, but the SRF Electron Linac is separate from the larger accelerator chain- including the Linac, Booster, Main Injector and assorted connected beamlines- and the collaborative nature of the facility at NML begs consideration of alternative control systems.

The first likely alternative was the Experimental Physics and Industrial Control System (EPICS) from Argonne National Laboratory (ANL). There have been some implementations of EPICS at Fermilab in the past, such as at the D0 collider experiment. D0 had been running exclusively with its own data collection infrastructure

written in Pascal on a VMS platform before a Platform Independence Decree between Collider Runs I and II. An implementation of EPICS, similar to ACNET in scope, is generally composed of a distributed network of computers that divide up the responsibility of running peripherals (magnets and other instruments), collecting readbacks, executing settings, and managing both through automated and end user programs. The biggest differences between ACNET and EPICS from an end-user perspective tend to come in the form of the development and implementation of the applications which depends almost exclusively on the resources dedicated to developing them. EPICS has always been intended as a generic control system, intended not only for use with accelerators, but also in other areas of research and even industrial applications - a fundamental point made in its name. With this comes one of its greatest advantages: a very large and varied base of users and developers making solutions to problems more likely found and solved quickly.

The other obvious ACNET alternative is the Distributed Object Oriented Control System (DOOCS) from the Deutsches Elektronen-Synchrotron (DESY) due to the collaborative nature of the accelerator at NML. CC2, a 1.3 GHz, 9-cell, TESLA-style cavity, would perhaps be reason enough considering that DESY had already developed a LLRF system, Simcon 2.1, and had developed the driver interface to DOOCS for their own use. DESY provided a set of Simcon 2.1 components which were successfully implemented on CC1 in 2005 and work was underway to develop Simcon 3.1, which would be able to control multiple cavities and could be used with CM1 and future cryomodules.

Consideration, however, must also be made to support and interface. In terms of the former, it was decided that maintaining support for DOOCS in the Accelerator Controls group just for the LLRF at NML was not a viable option. The latter also presents some challenges depending on whether the user is expected to work with multiple control systems or one control system interfaces with another for the user to work with. The first places higher demands on the user to learn the philosophies and nuances of different control systems, potentially confusion casual users, whereas the second places the burden on the hand-shaking between systems, potentially resulting in loss of settings and readbacks between systems. Instead of doing either for DOOCS, it was decided to use ACNET with LLRF developed in-house. Outside of LLRF, there were several controls written in EPICS, but these are largely deprecated in favor of the control and logging available through ACNET.

3.1.1 NML Clock

A localized system called NML Clock is used to coordinate timing between major components, such as the capture cavities and cryo modules, as well as their various sub-components. The triggers are coded as a 32-bit hex number from $00 to $FF that are generated in Node 654, the NML clock front end. At this time the $AB and $AC events are used to trigger the beginning of CC2 and CM2 pulses respectively. Timing for the pulses, including RF Gate delays, sample times, et cetera are at fixed times following these events.

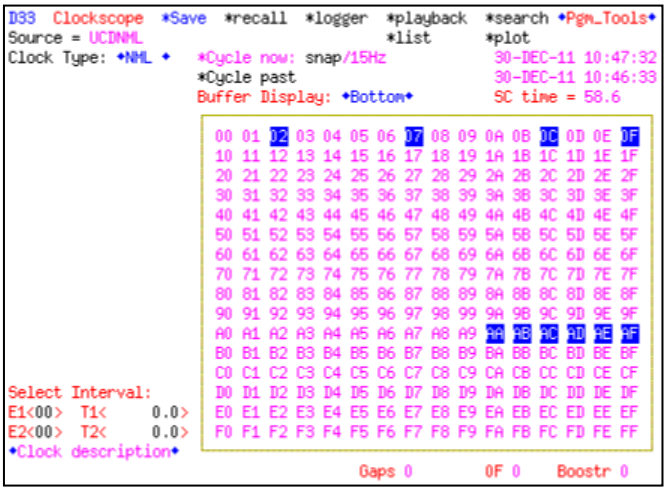

Figure 3-1. ACNET Clockscope page with NML clock selected.

The rate of the $AB and $AC is set locally and can be 0.2, 0.5, 1, 2, 2.5, 5, or 10 Hz by adjusting the Rep Rate Generator immediately above Node 654 in relay rack 215 at NML. The Rep Rate Generator pulses the $AB and $AC by referring to the periodic events ($A9, $AB, $AD, $AE, and $AF) that are locked to the Master Oscillator (MO), which is in turn line-locked. Note that the appropriate RF system should be turned off while switching and one should be mindful of the gradient that is being requested when turning back on at a different repetition rate, especially if moving to a faster rate. Running up to the same gradient at a higher repetition rate may result in a quench or other problems. A summary of NML clock triggers is in the table below.

Event	Description
$00	Super Cycle and Master Clock Reset
$02	Time Plot Timestamp Reset
$07	Poorly Line-Locked 720 Hz
$0C	15 Hz Booster Reset
$0F	Line-Locked 15 Hz

$8F	GPS-Locked 1 Hz
$A1	
$A9	MO-Locked 0.1 Hz
$AA	MO-Locked 1 Hz
$AB	CM2 Trigger
$AC	CC2 Trigger
$AD	MO-Locked 2.5 Hz
$AE	MO-Locked 5 Hz
$AF	MO-Locked 10 Hz

Table 3-1. NML clock event descriptions.

3.1.2 Synoptic Displays

To facilitate application development as well as to add some flexibility and a refined look to ACNET controls, Tim Bolshakov and Andrey Petrov of the AD Controls Department developed Synoptic, a Java-based Graphical User Interface (GUI). Unlike the separate control systems noted at the beginning of this section, Synoptic can most easily be thought of as an interface to ACNET. In general, settings and readbacks on the NML synoptic pages are attached to ACNET parameters, which can be adjusted and monitored independently in the event of a loss of communication between the Synoptic Server and the rest of the control system. Synoptic applications, called 'displays', are stored in a central repository as Extended Mark-up Language (XML) files. Displays can be launched a few ways:

- From an ACNET index page
- Through the synoptic web page, http://synoptic.fnal.gov/
- Through JAVA Web-Start

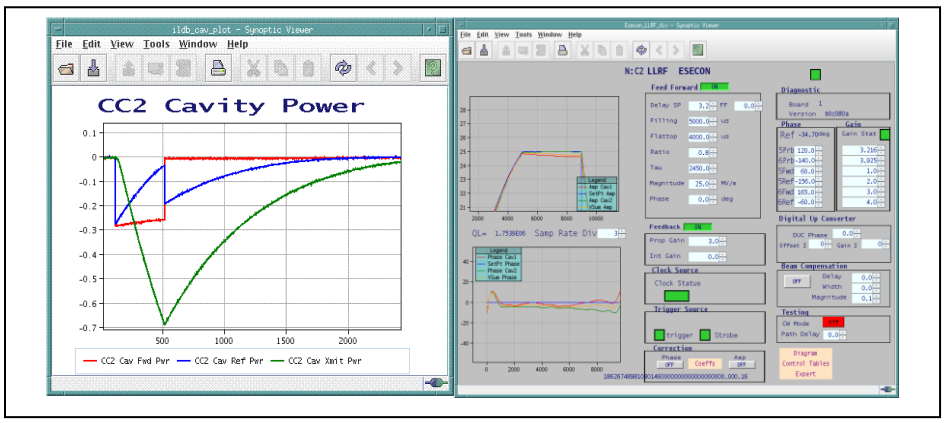

Figure 3-2. Synoptic displays are a way of graphically representing ACNET data.

These are not equivalent methods. The links through the synoptic web page display tree, in particular, do not allow for sets to be made in the control system and are generally most useful for monitoring only. The ACNET index page and the Web-Start will both bring up the display in the java viewer, which allows for settings to be made, but launching it from the ACNET index page will bring it up in the Linux console layer whereas launching it from the Web-Start application from the Windows layer will keep it in the Windows layer- most differences to the user there being cosmetic.

Unfortunately, there is no mechanism to maintain information on display authors or the date of the last update through ACNET index page and generally the information is not found on the Synoptic displays themselves. The easiest way to get such information is to find the display in the Concurrent Versions System (CVS) repository. At launch, the Synoptic display will appear something like the figure on the following page. A connection is made to the DAE server, but settings are initially disabled by default. To show this the DAE Connection Status indicator will be brown and anything associated with a setting will have an 'x' through it. To enable settings, one need only click on the DAE Connection Status indicator in the lower right-hand corner and select a period of time over which to keep settings active. Once done, the DAE Connection Status indicator will turn from brown to green and the 'x' will be removed from buttons and fields to show that settings can be made.

Anatomy of a Synoptic Display

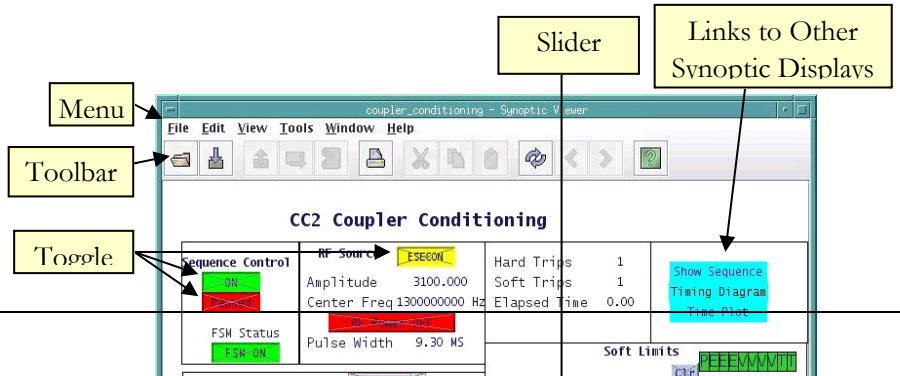

3.1.3 Front Ends

Front ends, not to be confused with the Front End (the NML beamline upstream of the first Cryomodule), are responsible for coordinating settings and readbacks to and from the various devices the operator wishes to control through ACNET parameters. ACNET parameters are generally named so that one may make a reasonable guess as to the function and physical location of the device that it controls. For a list of the accepted NML nomenclature one may refer to the naming convention primer. CMLLRF, for example, hosts a number of ACNET parameters in addition to providing the low level signal to the amplification chain for use in the cryo modules. These parameters may have any of a number of properties including analog setting, digital control, readbacks for either, and alarms for either. For example, N:M1FFA, hosted on CMLLRF, has an analog setting that an operator can use to adjust the amplitude of the system feed-forward to CM1 and a readback to verify that the front end acknowledges the current setting.

If a range of analog readbacks or a particular set of digital readbacks are desired, alarms can be set up to help the operator catch undesired changes. The NML facility has been assigned four alarm lists- **NMLUtl**, **NML_FE**, **NML_CM**, and **NMLMsc**- which each have a number of front ends associated with them summarized in the tables below. This means that if a parameter has analog or digital alarms properties and the 'Alarm List' field on D80 under the parameter summary for the parameter in question is 0 ('none'), then it will default to the alarm list associated with its host front end. It is important to note that, while the consoles at NML have their alarm screens monitoring these lists, other consoles around site will generally not and the operator will have to edit their alarm screen properties through D6 to monitor NML alarms. This can be done in a few easy steps as shown in the figure to the left.

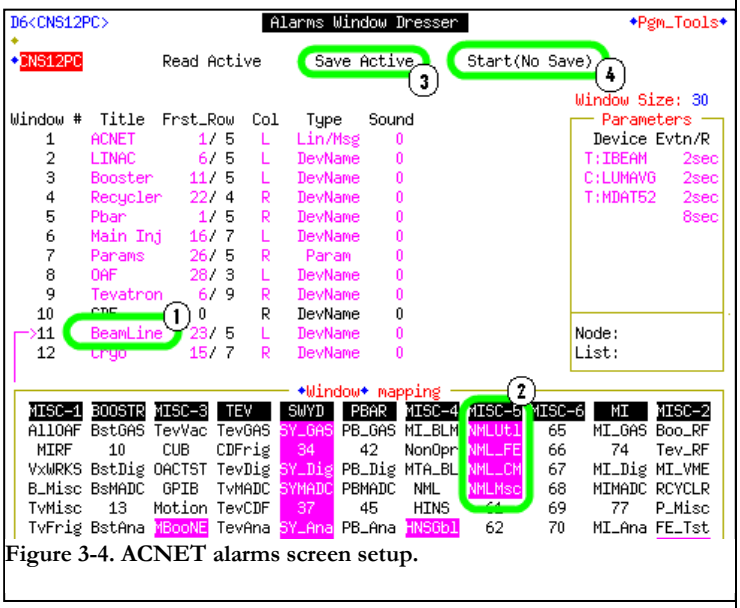

Figure 3-4. ACNET alarms screen setup.

- Click an appropriate list.
- Select the alarm lists.
- Click 'Save Active'.
- Click 'Start (No Save)' to restart the alarm screen.

Most of the front ends are local to NML, but there are a few exceptions listed below. The need for these exceptions is either that it is a development front end and not essential to NML, or it is shared between systems. The latter group consists of the NMLOPC process, which runs on DCE45, NMLRF1, which handles EPICS to ACNET bridging for both NML and HINS, and the MOOC/PEP bridges used primarily to interface with the 5 MW Klystron system. There are also several calculated parameters updated by MACALC, an OAC for calculations that runs on DCE10 in the Cross Gallery computer room. Power outages in those areas and other disruptions will affect settings to and readbacks from those front ends.

Name	Type	Location	Alarm List	Description
BADMAB	VME	TGS-120		MOOC/PEP Bridge
BADMB2	VME	TGS-120		MOOC/PEP Bridge
CMLLD	VXI	TGC-200	NMLMsc	CM LLRF Development
NMLOPC	ALIAS	MAC Room	NMLUtl	Cryo Equipment Interface
NMLRF1	VME	BTE-213		NML and HINS Epics Bridge
PXIC13	PXI PC	IB1-MW025		NML Resonance Control Test

Table 3-2. Partial list indicating the front end name and associated information.

Local front ends control various components of the beamline and interact with the rest of the control system to provide readbacks and act on changes requested by the

Name	Type	Location	Alarm List	Description
CC2LLR	VXI	Rack 247	NML_FE	CC2 Simcon LLRF
CMLLRF	VXI	Rack 268	NML_CM	CM1 LLRF
MSPC24	PC	Rack 241	NMLMsc	Seismic Monitor
NMGWIL	VME	Rack 288	NML_FE	NML Gun/Window Interlock
NML654	IRM	Rack 215	NMLMsc	NML Clock Generator
NML655	IRM	Rack 242	NML_FE	CC2 Timing & DAQ
NML656	IRM	Rack 279	NML_CM	CM1 Timing & DAQ
NML657	IRM	Rack 215	NMLMsc	General DAQ
NMLA	VME	Rack 211	NML_CM	Motor Controller

NMLGP1	VME	Rack 210	NMLMsc	General Purpose
NMLGP2	VME	Rack 210	NMLMsc	General Purpose
NMLHOM	VME	Rack 219	NMLMsc	HOM Readout
NMLLRF	VME	Rack 247	NML_FE	CC2 LLRF
NMLRFI	VME	Rack 277	NML_CM	CM1 Klystron Interlocks
NMLVAC	VME	Rack 214	NMLUtl	NML Vacuum
NMLVM1	VME	Rack 245	NML_FE	CC2 Klystron Interlocks
NMLWPM	VME	Rack 289		Wire Position Monitor
PXIC16	PXI PC	Rack 252	NMLMsc	LFD Compensation Controller
PXIC21	PXI PC	Rack 253	NMLMsc	SRF Cavity Test
UCDNML	VME	Rack 210		Universal Clock Decoder
HLS-NML-1	PC	Rack 264		Hydro-Leveling System

user or other processes. These are located throughout NML in the relay racks noted in the table below. All of these can be found on D31 by searching for or typing in the name in the node poll list except for HLS-NML-1, which is not yet integrated into the ACNET control system.

3.1.4 Lorentz Force Detuning

Lorentz Force Detuning (LFD), a significant problem with higher gradient cavities, adds to the list of other problems that are prevalent specifically in SRF including microphonics and ponderomotive effects. Unlike the others in the list, however, LFD changes rapidly though a pulse as the gradient of the cavity is raised to a flat-top level before being removed from the cavity. To compensate, a program has been put into place to record the LFD response from the cavity and compensate for it using piezo tuners, which can act quickly enough to stabilize the detuning and keep the cavity at its resonant frequency of 1.3 GHz. The mechanism for performing the LFD compensation is currently a Matlab application that retrieves data through a backdoor method on the LLRF front end, performs a number of transforms to the data and then

applies a calculated compensation curve to the cavity piezos. For the time being this program must be run manually. To start it, one need bring it up on a remote desktop by performing the following steps.

Run a remote desktop to **pxic16.fnal.gov**, or alternatively to its IP address of **131.225.142.38**. You must be on the proper side of the firewall to access it so those trying to access it from outside control rooms will have to go through Beams-TS or another proxy.

Log in with your Windows Services username and password. If another session is already in progress then a reboot the PXI PC labeled PXICONT22 in relay rack 252 will be required to allow a new user to log in. This should be done cautiously since the other account may be running the LFD compensation controller.

Once logged in, run the "Matlab RemoteDesktop" shortcut. Matlab will start and default to the Matlab folder, as seen at the top-center of the window.

Browse to **C:\NML_DAQ\LabView**

Type **lfdcontroller** at the command line prompt in the main window to bring up the NML Lorentz Force Detuning Controller window.

If the cavity has changed significantly a scan may be required but otherwise it should be skipped. To perform this click **Scan** under the LFD menu. This will take several minutes to sweep through a range of biases and send a bias ping across the RF pulse to measure the response.

Compensation can be turned on by clicking **Compensate** under the LFD menu. It will apply the compensation curve from the last scan, which should get the piezos close.

Once compensation is active, adaptive compensation can be turned on by clicking **Adapt** under the LFD menu. This updates the compensation curve from pulse to pulse and within the pulse to make for a better match to small changes in the cavity brought on by changes in gradient, tune of the cavity, loaded Q of the cavity, changing microphonics, etcetera.

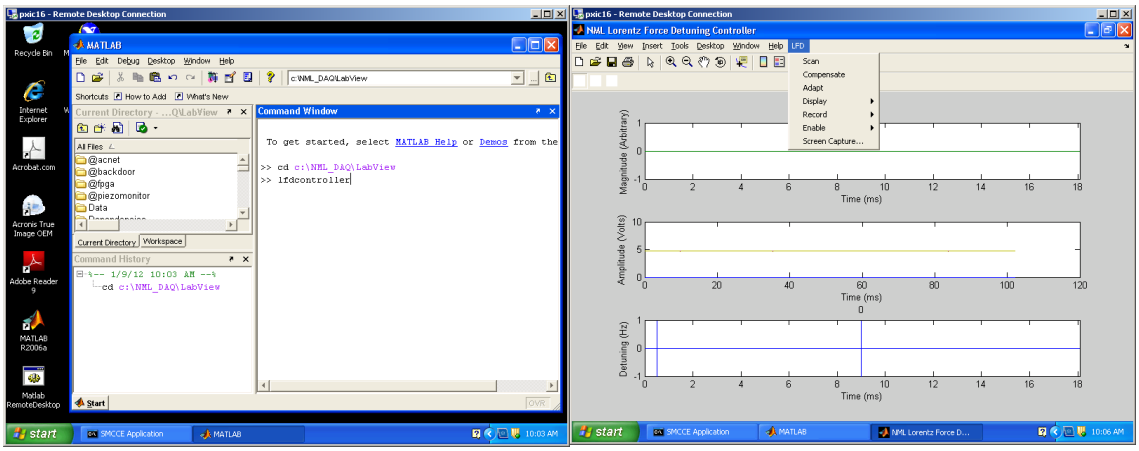

3.2 Machine protection system

The Machine Protection System (MPS) was developed in stages that were commensurate with the commissioning goals for the FAST beamline. The primary objectives, from the MPS point of view, are to mitigate beam induced damage to the machine components and to provide a comprehensive over-view of the entire accelerator based on the input status of all the relevant subsystems.

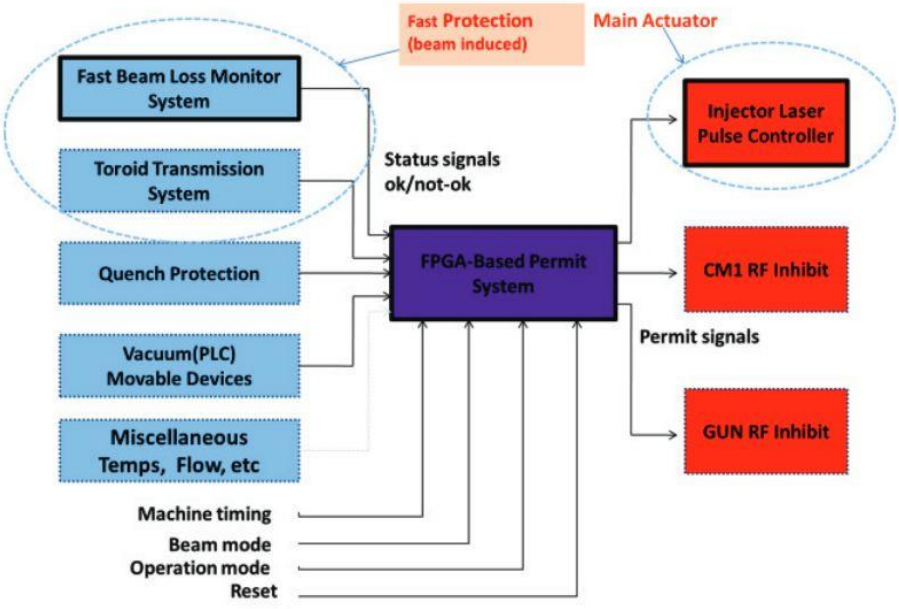

Figure 5: MPS overview.

Figure 26 illustrates the overall MPS design which is divided into 3 layers; a sensor layer to collect subsystem status, a process layer that utilizes the status to generate the permits and an actuator layer to receive the permits and inhibit the beam. The initial stage of this development involves the design of the Laser Pulse Controller (LPC).

3.2.1 Laser pulse control

The backbone of the FAST facility is a radio frequency (RF) photo-injector. The electron source is a 1-1/2 cell cylindrical-symmetric RF gun with a Cs_2Te photocathode. The cathode is illuminated by an ultraviolet (UV, λ=263 nm) laser pulse produced via frequency quadrupling of an amplified infrared (IR, λ=1054 nm) pulse [3]. The photocathode drive laser enables the generation of a train of bunches repeated at 3 MHz within a 1 ms duration. The 5 MeV electron bunches exiting the RF gun are then accelerated with two superconducting radio-frequency (SRF) TESLA-type cavities (CC1 and CC2) to approximately 50 MeV. Thus, one of the main actuators for the MPS is the injector Laser Pulse Controller (LPC). This device is designed to control the number and the spacing of bunches in a macro-pulse by picking single laser pulses out of a train; achieved by manipulating the Pockels cell (voltage-controlled wave plates). The LPC, basically, provides a gate, the length of which determines how many 3 MHz laser pulses are accepted. The gate widths (minimum through maximum), delay (relative to RF), and timing for first bunch trigger along with several other parameters are configured via the control system. The maximum allowed duration for the gate is 1 ms. Figure 2 illustrates this scheme diagrammatically.

This system is also the main actuator for beam inhibits issued by the MPS. It is built on a VME platform with a fully programmable general purpose FPGA board. It has inputs for the requested beam modes (intensity limits) defined by the logic layer of the MPS, the MPS permit signal, the 3 MHz machine timing, and for a macro-pulse trigger. It has control outputs for the Pockels cell driver, a mechanical shutter and a first bunch timing signal. From the protection system point of view the pulse controller is used to:

- Block the Pockels cell based pulse kickers while the MPS input is in an alarm state.
- Enforce the limit on the number of bunches as given by the currently selected beam mode.
- Close the laser shutter on request of the MPS.

This may happen when there is no valid operational mode or when some combination of loss monitors exceed set thresholds which trigger a dump condition. Note that this

minimum setting is the default number of bunches allowed and is designed to meet shielding requirements as well as to force operation below the threshold for machine damage potentials.

The MPS includes a fast protection system that is based on 40 Beam Loss Monitors (BLMs). It is designed to interrupt the beam within a macro-pulse and relies heavily on the ability to detect and react to losses within a few nano-seconds; the loss monitors are made from plastic scintillator material and are coupled to photomultiplier tubes. First injector beam test, Figure 3, with these loss monitors indicate that the monitor possess the necessary sensitivity required to detect low charged losses as well as dark current.

These BLMs will serve the dual purpose as an accelerator diagnostic and as the primary detectors for fast machine protection. The monitors must therefore deliver a measurement of beam and dark current losses to the control system as well as generate a fast alarm signal when the beam losses exceed user-defined thresholds. The time resolution of the loss measurement must provide the ability to distinguish single bunches within each macro-pulse. This requires a sampling frequency of at least 3 MHz with a repetition rate of 5 Hz. The BLMs are being integrated into a beam loss monitoring system capable of generating a fast trip signal based on a programmable fast comparator setting as well as an alarm condition that is derived by comparing the outputs of the PMT signals with various programmable thresholds within the BLM electronics. This alarm output is a critical component for machine protection. The desire is to provide a machine protection trip well before the beam can damage accelerator components. If one of the programmed thresholds is exceeded or if an error condition such as a high voltage failure or failed monitor is detected the system should report this to the MPS logic which in turn reduces the intensity or inhibits the beam via the LPC. The main requirements for the BLM system are:

- Provide both machine protection and diagnostic functions.
- Instantaneous read-back of beam loss
- Digital output for integrating and logarithmic signal (16 bit)
- Built in self-test and on-board signal injection for testing of monitors between pulses.
- FPGA controlled
- Local data buffer
- VME interface to ACNET control system
- Continuous and pulsed monitoring

- Wide dynamic range

Figure 4 is a simplified diagram of the signal processing path and the controls interface of the loss monitor electronics. A 125MHz digitizer board provides digitized signals and contains 512 MB of on-board RAM used for data logging.

3.2.2 Controls integration

Controls integration is a key component of the MPS design concept as it not only ensures system reliability, but also allows for post-mortem analysis of detected trips. A PowerPC 5500 series board was chosen as the slot 0 controllers for the various MPS hardware components including both the LPC and BLM systems. These boards run at 1GHz, have over 1GB of expandable Ram and provide the reading and setting interface to the ACNET control system. Figure 6 illustrates the General Purpose FPGA board (V1495) that serves as the backbone for both the LPC and the main MPS system. This board handles all of the real-time computing required at the hardware level. A daughter card has been designed for the V1495 board that provides 128-MB of SDRAM. This memory extension is crucial as post-mortem fault analysis will require extensive buffers to log sensor readings around a detected fault. The daughter card includes an additional FPGA that is used as an interface and a SDRAM controller. The data path between the daughter card and the main MPS FPGA board is 32 bits wide. If running at 62.5 MHz, the peak through-put is 250 MB/s. Figure 6 shows a block diagram of this card and interface to the main MPS board.

SECTION 4

UTILITIES

4.1 Low Conductivity Water System

The LCW system at NML is designed to remove heat from critical components. The LCW supply temperature is regulated to 90 ±1 degrees F. The maximum flow is 1000 gpm and the maximum pressure is 115 psig. The resistivity is kept at 4 MΩ with a dissolved oxygen level of 20-60 ppb.

Figure 1. Variable frequency drive LCW pump (left) and heat exchanger (right).

There are three 500 gpm LCW pumps, of which, one is kept on and two remain in reserve. The LCW heat exchanges with a 60% Water/40 % Propylene Glycol Chiller system. The chiller unit has a 180 ton (633 kW) capacity and a water delivery of 354 gpm at 63 degrees F.

Figure 2. VFDs are on the wall outside and adjacent to the pump room (left). The chiller is on the northeast side of NML (right).

LCW is pumped through an oxygen removal skid that is capable of maintaining a 20 to 60 ppb ratio. Distilled water is used for making up water to the LCW system.

Figure 3. The oxygen removal skid is located at the northwest corner of the pump room. The reservoir tank is mounted on the east wall of the pump room.

The LCW system is controlled by the Main Control Panel, which sits left of the pump room doors, prior to entering the room. There are 3 displays on the panel. The largest display is the Eaton PanelMate PLC controller which provides LCW system status, and allows for pump control, trip resets, and trip limit settings.

Figure 4. The image on the right is the Main Control Panel. The left image shows the loop controllers on the front of the Main Control Panel.

In Figure 4, the top right PID controller is for LCW temperature regulation. The temperature set point and loop control parameters are adjusted with this controller. The top left display is the dissolved oxygen analyzer, which returns data from the oxygen removal skid.

The RF Gun skid heat exchanges with the LCW system since the greatest allowable temperature deviation is 0.1 degrees F. Greater temperature swings would take the RF Gun cavity off resonance due to volume variations. The skid is located behind the Laser Room, in the south tunnel. The RF Gun cavity, Main and Bucking solenoid magnets, and RF coupler are cooled from this skid.

4.2 Instrument air

Dry compressed air is needed for manipulating cryo valves, vacuum valves, and pneumatic actuators. There are 2 air compressors located in the first floor central east-side room that supply compressed air to the entire building. One compressor is on at all times with the other in standby. If the main compressor should fail, then the other will turn on and maintain the proper pressure. The system maintains a supply pressure between 110 and 112 psi. The FAST Cave west wall supply for the Low Energy Beamline is set to regulate to 108 psi, any lower and actuator devices may slowly creep into the beam path.

Figure 5. Pneumatic actuator installed on the 9-way cross during assembly.

4.3 Vacuum system

The vacuum system is comprised of the Photocathode transfer system, RF Gun, Diagnostic table, 50 MeV beamline, CC1 beamtube and cryostat, CC2 beamtube and cryostat, CM2 beamtube and cryostat, and the 300 MeV beamline. The beamtube vacuum utilizes ion pumps and the vacuum is maintained at 1e-10 Torr.

The ion pump power supplies and controls for the Photocathode transfer, RF Gun, Diagnostic table, CC2 beamtube and cryostat, and CM-2 beamtube and cryostat are located in relay rack 212, 213, and 214. The 50 MeV beamline vacuum system supplies and controls are located in relay racks 241.

4.4 Electrical

The majority of NML power is supplied through circuits 15-A and 15-C. The 15-A and 15-C main breaker panels are located in the Instrumentation Room, northeast corner of NML. The former Computing Division room on the first floor of NML utilizes circuit 15-B which is located inside the room. The circuit 15-B will be decommissioned after the FAST-IOTA control room is relocated to the first floor.